Experimental and Theoretical Investigations of Functional Supramolecular Assemblies

A Thesis

Submitted in partial fulfillment for the degree of

Master of Science

as a part of

Integrated PhD programme (Materials Science)

By

Chidambar Kulkarni

CHEMISTRY AND PHYSICS OF MATERIALS UNIT

JAWAHARLAL NEHRU CENTRE FOR ADVANCED SCIENTIFIC RESEARCH (A DEEMED UNIVERSITY)

Bangalore-560064, India

MARCH-2011

DECLARATION

I hereby declare that the matter embodied in the thesis entitled "**Experimental and Theoretical Investigations of Functional Supramolecular Assemblies**" is the result of investigations carried out by me at the Chemistry and Physics of Materials Unit and New Chemistry Unit, Jawaharlal Nehru Centre for Advanced Scientific Research, Bangalore, India under the supervision of Prof. S. Balasubramanian and Dr. Subi J. George and that it has not been submitted elsewhere for any degree or diploma.

In keeping with the general practice in reporting scientific observations, due acknowledgement has been made whenever the work described is based on the findings of other investigators. Any omission that might have occured by oversight or error of judgement is regretted.

Chidambar Kulkarni

CERTIFICATE

I hereby certify that the matter embodied in the thesis entitled "**Experimental and Theoretical Investigations of Functional Supramolecular Assemblies**" has been carried out by Mr. Chidambar Kulkarni at the Chemistry and Physics of Materials Unit and New Chemistry Unit, Jawaharlal Nehru Centre for Advanced Scientific Research, Bangalore, India under my supervision and that it has not been submitted elsewhere for the award of any degree or diploma.

Prof. S. Balasubramanian
(Research Supervisor)

Dr. Subi J. George
(Research Supervisor)

Dedicated to

Parents

Acknowledgements

It gives me immense pleasure to thank both of my research supervisors, Prof. S. Balasubramanian and Dr. Subi J. George for allowing me to work on both ends of the spectrum, from experimental to computational chemistry. I thank them for the encouragement, support and guidance provided to me, both academic and non-academic wise throughout the course of my research. I acknowledge the academic freedom that I enjoyed in their lab during the course of this work. I thank them for providing excellent experimental as well as computational resources without which this project would not have been successful. The infectious enthusiasm of both the supervisors towards science has kept me motivated throughout the course of project.

I thank Prof. C. N. R. Rao, FRS for sharing his research experiences and for narrating us motivating scientific anecdotes on various occasions in JNCASR and IISc.

I would also like to thank Prof. G. U. Kulkarni, Chairman, CPMU for providing excellent research facilities.

I express my sincere thanks to various faculty members of JNCASR and IISc for their courses. I would like to thank Prof. S. Balasubramanian, Prof. S. K. Pati, Dr. N. S. Vidhyadhiraja, Prof. A. Sundaresan, Dr. T. K. Maji, Dr. M. Eswaramoorthy, Prof. S. Narasimhan, Prof. U. V. Waghmare, Prof. S. M. Shivaprasad, Prof. G. U. Kulkarni, Prof. K. S. Narayan, Dr. S. J. George, Dr. T. Govindaraju, Prof. N. Chandrabhas, Dr. Ranjan Datta, Mrs. Shoba from JNCASR and Prof. Ranganathan and Prof. P. Balaram from IISc, for the various courses which were extremely helpful to me.

It gives me great pleasure to thank my lab mates starting with Ankit Jain, Mohit Kumar and Venkat Rao for teaching me the art of organic synthesis and also for many fruitfull discussions on varied subjects. I would also like to thank other newer members of lab like Bhawani N, and summer research students for their support and help. I would like to thank the wonderful bunch of labmates from the computational lab : Srinivas Raju, Sandeep Kumar Reddy, Saswati

Sarangi, Bharat Rajeshwaran, Rajdeep Singh Payal, B. Satyanarayana, Kanchan and Dr. Ganga Periyasamy for their invaluable suggestions and support throughout the course of the project. I would also like to thank all the labmates from experimental as well as computational lab for sharing some of the wonderful moments out of lab.

I am privileged to have wonderful batchmates with varied talents : Arpan, Gayatri, Sharma, Sudeshna, Rana, Varun, Dileep and Pandu. I thank them for all the help and friendship and also for some of the memorable moments.

I would like to thank Mahesh, Selvi, Roopa and Sonia for helping me in various characterisations.

I am thankful to the open source community for providing useful softwares. In particular I would like to acknowledge the developers of VMD, CPMD and LAMMPS.

I am thankful to the staff of CCMS for the computational facility and also to JNCASR for the excellent research facilities and stimulating ambience.

I also thank Department of Science and Technology for the financial support.

Finally I would like to thank my parents and friends for being there through my ups and downs.

Synopsis

This thesis has two parts, with the first concerning about the experimental studies on supramolecular assemblies and the second is about the mechanisms of supramolecular polymers. The first part deals mainly with the chemistry of coronene imides, their synthesis and self-assembly. The second part deals with the mechanisms operative in the supramolecular family of benzene-1,3,5-tricarboxamides.

Part A has three chapters, first chapter gives an introduction to the field of supramolecular chemistry, its recent developments and self-assembly of π conjugated systems leading to multichromophoric systems for varied applications. The first chapter illustrates the use of multichromophoric systems approach coupled with self-assembly to yield more fruitful applications.

Chapter two is concerned with the synthesis of a new electron withdrawing chromophore, coronenetetraimide. Our approach here involved the use of Diels-Alder reaction under microwave conditions and also we have shown another approach through which the yield of the synthesis is expected to be much higher. We envisage that this chromophore can have potential applications in photovoltaic devices.

Chapter three deals with the synthesis and self-assembly of new Donor-Acceptor-Donor triad involving coronene bisimide as the acceptor. This chapter explains the synthesis and the preliminary results on self-assembly and morophological studies of this molecule.

Part B consists of two chapters, first chapter gives an introduction to the field of supramolecular polymers and different mechanisms involved in the polymerisation. It also gives an introduction to the theoretical aspects which are used to study the polymerisation mechanisms.

Chapter two deals with the mechanism of supramolecular polymerisation in the family of benzene-1,3,5-tricarboxamides (BTA). Here using different computational techniques we have shown that a subtle change in the intermolecular interactions leads to a change in the mechanism of self-assembly in this family. The importance of intermolecular hydrogen bonding to direct the mechanism of self-assembly is shown.

CONTENTS

Part B Theoretical study of supramolecular polymerisation in Benzene-1,3,5-tricarboxamides

1. Introduction

2. Cooperativity in the stacking of Benzene-1,3,5-tricarboxamides

PART A

SYNTHESIS AND SELF-ASSEMBLY STUDY OF CORONENE BASED IMIDES

Chapter 1

Introduction

Abstract

With the discovery of conducting polymers in the late 1990s the field of organic electronics has seen an enormous activity from a range of researchers including chemists to physicists. As the physics and chemistry of these polymers are being understood and appreciated, an emerging field of oligomer or small molecular electronics has taken birth. Assembling these oligomers using non-covalent interactions which are so ubiquitously found in nature, chemists have contributed immensely to small molecular approach to electronics. The assembly of these small molecules is important because, the performance or the efficiency of the organic electronic devices depend not only on the molecular structure but also on its organisation in the active layer of the device. In this chapter an introduction is given to the supramolecular chemistry and its use in assembling small functional molecules to obtain self-assembled systems and their applications in molecular electronic devices as reported in literature.

1.1 Historical background

Supramolecular chemistry is defined as the “ chemistry beyond the molecules ” or “ chemistry of non-covalent interactions ” . This branch of chemistry came into recognition with the pioneering work of Donald Cram, Jean-Marie Lehn and Charles J. Pederson in the late 1970s. C. J. Pederson accidently found that cyclic polyethers formed stable complexes with alkali and alkaline earth metals.[1] Although the synthesis and presence of these cyclic polyethers was known much before Pederson and coworkers,[2] the connection between these structural motifs and the molecular recognition was first brought about by D. Cram, J. M. Lehn and C. J. Pederson. This opened up a whole new branch of chemistry called “Supramolecular Chemistry”. As with any new area of science, early research in this field was driven primarily because of curiosity rather than any other application or higher goal. By the late 1980s the connection between these ideas and the forces operative in natural systems started becoming evident. Thus new concepts of host-guest chemistry came into picture and molecular recognition was much more mature as a concept. According to J. M. Lehn the subject can be broadly divided into two subclasses which are connected in some sense namely, supermolecular assemblies and the supramolecular assemblies. The former consists of well-defined, oligomolecular species formed by specific intermolecular interaction of few components based on the principles of molecular recognition. The latter consists of multicomponent systems having multiple interactions resulting in spontaneous self-assembly leading to well-defined microscopic organisation forming different structures depending on the functionality present in the building units.[3] Over the past two decades because of the potential applications of these functional supramolecular systems, a paradigm shift is seen in the supramolecular research from conventional

host-guest supramolecular chemistry to functional self-assembled systems.

The beauty of the subject lies in the handle provided by the non-covalent interactions, most of which are weak thus can be used reversibly. Although each individual forces are weak, in synergy they can be quite strong to direct a particular organisation, this is termed as cooperativity.[4] This synergy and organisation is exemplified by the way nature works. Most of the complex natural systems such as lipid bilayer assembly, the DNA double helix, the collagen triple helix, photosynthetic assembly and the tertiary and quaternary structures of proteins are all formed by non-covalent interactions. Thus using these tools we can mimic nature and even we can find solution to our energy crisis by developing supramolecular artifical photosynthetic systems.[5]

1.2 Non-covalent interactions

Non-covalent interactions form the cornerstone of supramolecular chemistry. These include electrostatic interactions (ion-ion, ion-dipole and dipole-dipole), hydrogen bonding, π-π stacking interactions, solvent effects and van der Waals or dispersive interactions (Table 1.1). These interactions can be either attractive or repulsive. In many cases a multitude of these interactions act together, albeit one takes predominance over others.[6]

Interaction	Strength of interaction (kJ/mol)
Ion-Ion	100 to 350
Ion-Dipole	50 to 200
Dipole-Dipole	5 to 50
Hydrogen bonding	4 to 60
π-π stacking	4 to 20
van der Waals	5 to 10

Table 1.1 Various non-covalent interactions and their respective strengths.

Among the electrostatic interactions ion-ion interactions are the strongest and they result from attraction or repulsion of charges on ions. An example of this type is the complex formed between tris(diazabicyclooctane) host (positively charged) and that of $[Fe(CN)_4]^{3-}$. These are not encountered frequently in most supramolecular structures and since these are very strong less flexibility for the reversal of interaction. The ion-dipole interaction is between an ion and the corresponding head of the dipole. Classic examples of this type are the complexes formed between alkali or alkaline earth metals and cyclic polyethers. Dipole-dipole interactions arise when two dipoles are aligned to show either attractive or repulsive behaviour. These are long range interactions which decay as the third power of distance between them (assuming point dipoles). These interactions are mainly observed in chromophores stacking and self-assembly. The strength of electrostatic interactions strongly depend on the nature of the solvent in which they are operating.

Hydrogen bonding is ubiquitously found in nature. It is because of the presence of hydrogen bonding in water and DNA base pairs, life on earth is possible. Thus it is no wonder that hydrogen bonding forms one of the most crucial interactions. A hydrogen bond D-H-----A, is formed between a hydrogen atom attached to a electronegative donor (D) atom and a neighbouring acceptor (A) atom bearing lone pair of electrons. The strength of hydrogen bonding can be increased by using multiple hydrogen bonds in a correct geometrical arrangement. Hydrogen bonding is also a special kind of dipole-dipole interaction possessing directionality.

π-π stacking interactions are weak, short range interactions, arising mainly from the induced dipole-induced dipole interactions. The study of stacking of benzene has got a lot of attention because it is the simplest analogue of many higher conjugated carbon materials and also because of the presence of DNA base pairs consisting of such motifs. It is shown by high level quantum

chemical calculations that face to face geometry is slightly repulsive and many slipped or T-shaped geometries are more favourable energetically. The stacking geometry for a particular π-conjugated system depends on the substituents and the solvents in which they are being studied.

Dispersive or van der Waals interactions and solvent effects are also very weak in terms of their strength. But they do have a significant say in the assembly of supramolecular systems. Given the nature of the solvent, they dictate the assembly into different morphologies.[7]

1.3 Self-Assembly by specific intermolecular interactions

Controlling the self-assembly of synthetic, multicomponent systems using non-covalent intermolecular interactions is at the heart of the supramolecular chemistry. This approach provides an excellent handle to manipulate systems at the nanoscale and also a control over the functional properties at the macroscopic level using subtle variations of interactions. These interactions have been used to obtain a plethora of architectures such as vesicles, nanotapes, intertwined helices, nanorods, random coil polymers and many more. Another feature of these self-assembled systems is the dynamicity of the assemblies. Better understanding of this dynamic nature in terms of molecular features paves way for constructing more complex assemblies with desired functions.

A range of molecules or systems can be chosen for self-assembly, depending on the application in mind. π-conjugated systems turn out to be the best choice for electronic applications. The self-assembly of π-conjugated systems mainly uses hydrogen bonding,[8,9,10] π-π interactions,[11] amphiphilic interactions[12,13] along with others like ligand-metal interactions.[14] These can be used to assemble molecules in solutions and on surfaces.

1.4 Multichromophoric systems

Chromophores are conjugated molecules capable of absorbing light and thus exhibiting colors. Nature has organised many chromophores with elegance using non-covalent interactions to generate photosystems. The self-assembly of synthetic multichromophoric systems can be used in supramolecular electronic devices to mimic natural photosynthetic systems and they can also be used to study the fundamental processes of electron transfer and energy transfer operating in photosystems.[15,16,17] In supramolecular electronics the size of the self-assembled active component is around 5-20 nm.[18,19] Because of their assembled nature they can provide better charge transport reducing trap sites which are present in conventional polymer devices. But this approach also has its own challenges like transferability of the assemblies from solution to devices with almost perfect alignment.

Inspite of all the challenges, many chromophores (Figure 1.1) have been used to build functional multichromophoric systems. A large amount of literature on multichromophoric systems stems from the groups of Klaus Müllen,[20,21,22,23,24,25,26] Jean M. J. Fréchet[27,28,29,30] and Michael R. Wasielewski.[31,32] While Müllen's group concentrated mainly on the photophysics of these systems and development of new polyphenylene systems, Fréchet's group came up with new dendrimer based systems for cascaded Förster Resonance Energy Transfer (FRET) and light harvesting. On the other hand Wasielewski's group aimed at rylene diimides and porphyrins for artifical photosynthetic systems and their self-assembly along with the study of the photophysics. Apart from these, there is a significant contribution from other groups as well involving other chromophores.[33,34,35,36,37,38,39]

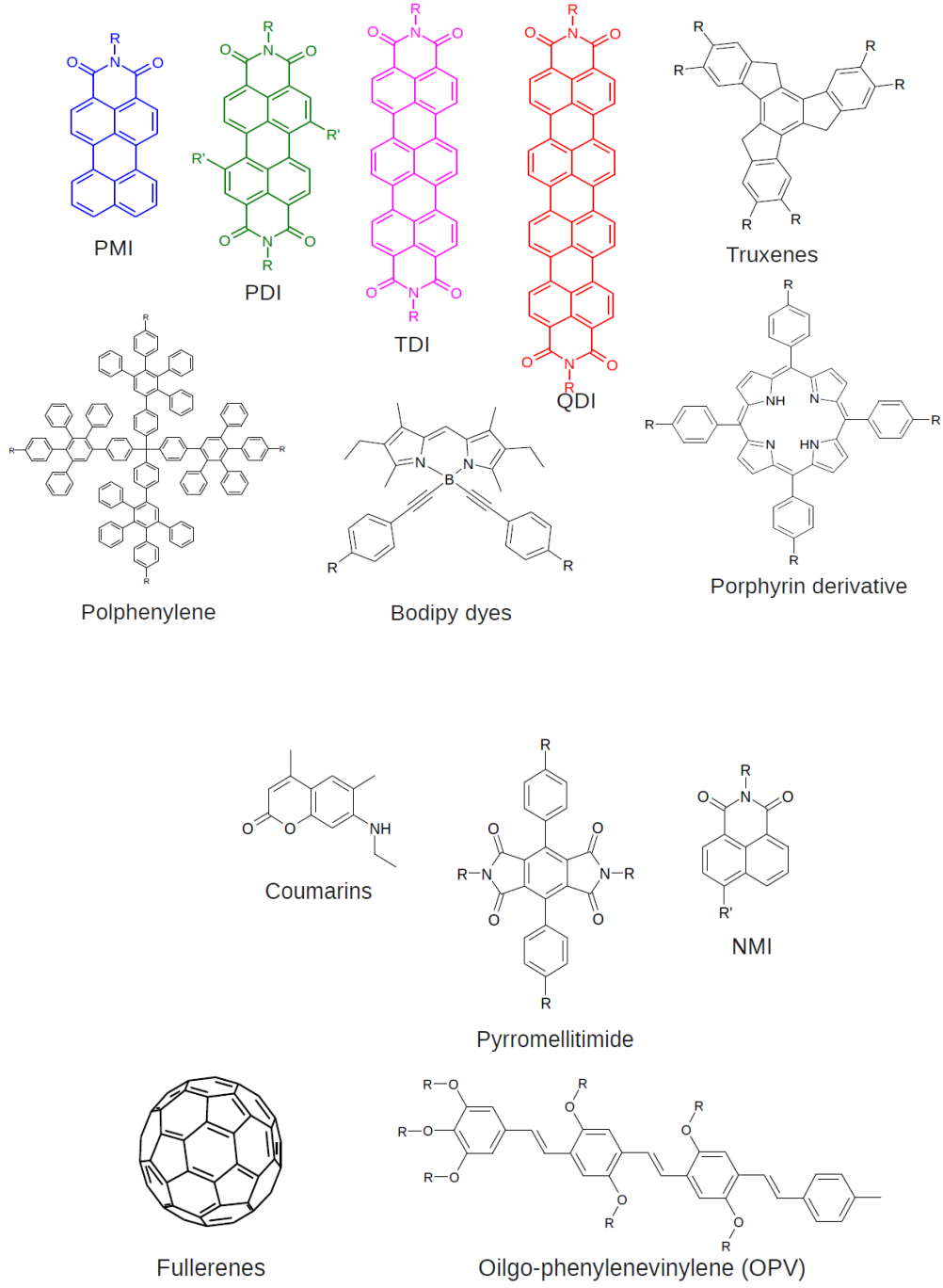

Figure 1.1 Structures of different chromophores reported in literature.

Some of the early multichromophoric systems were used for cascaded energy transfer and light harvesting, with the main contribution coming from J. M. Fréchet's group. The rule of thumb for the design of multichromophoric systems for energy transfer are (1) Spectral

matching between different components of the systems (2) Orientation of the different components and (3) Central core bearing multiple attaching sites. To fulfill the above criteria dendrimers turned out to be the best choice. In a multichromophoric dendrimer, many chromophores are arranged to achieve efficient energy transfer. The below schematic (Figure 1.2) shows a typical multichromophoric dendrimer (**1**) for energy transfer. Different colors indicate different chromophores in **1**.

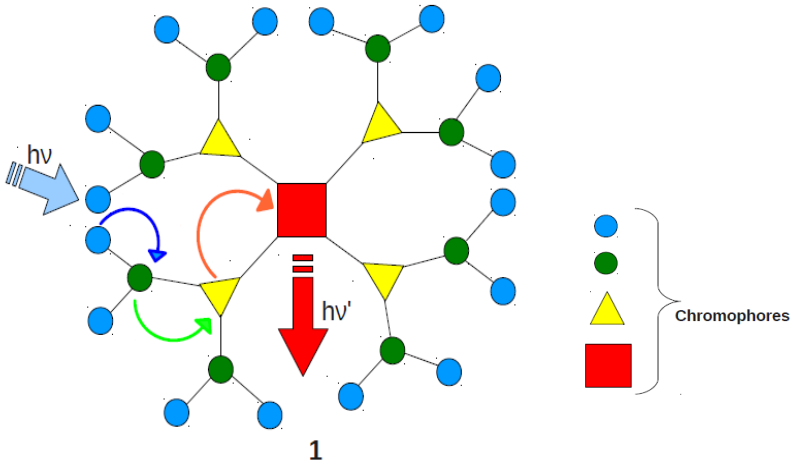

Figure 1.2 Schematic of multichromophoric dendrimer.

A typical example of a functional dendrimer which is a potential light harvesting system consists of a porphyrin core and napthopyranone donor as the first generation and coumarin donors as the last generation (Figure 1.3).[40] This was synthesised by an elegant deprotection and esterification cycles. It consists of 25 chromophores, absorbing in the most part of UV and visible region. Also the emission ranges from 625 nm to 750 nm (Figure 1.3). It was observed that irrespective of excitation of whichever donor, the emission resulted only from porphyrin indicating near quantitative energy transfer. Also many other multichromophoric functional dendrimers are reported for energy transfer.[41,42] Most of them involve the same concept of arrangement of chromophores leading to vectorial or directional energy transfer.

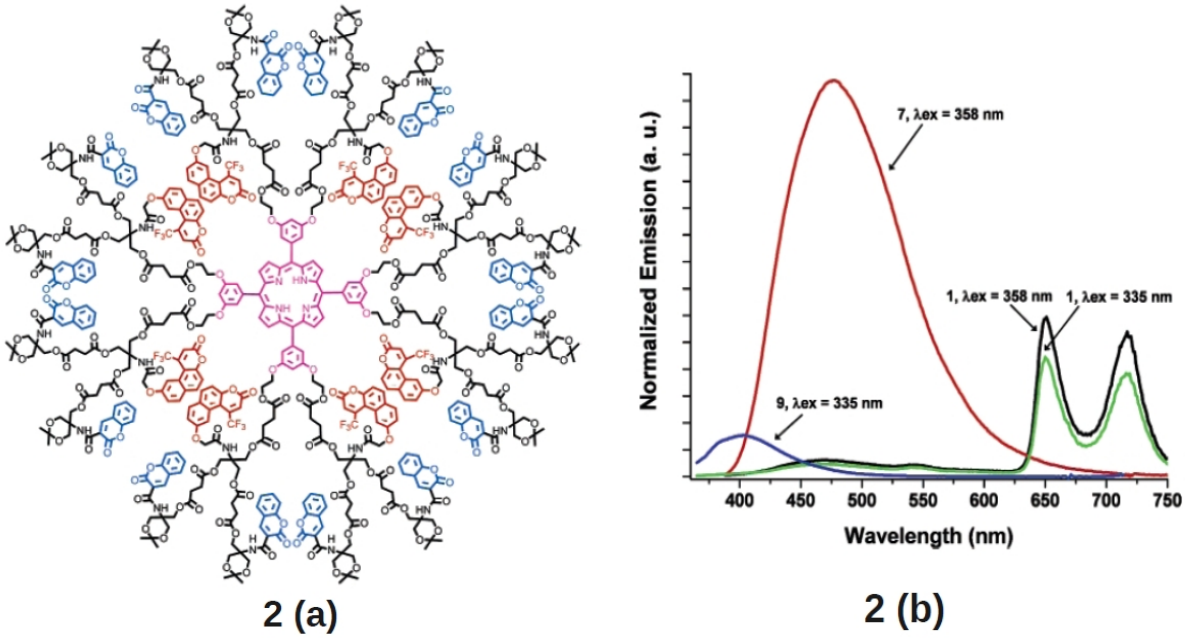

Figure 1.3 Multichromophoric dendrimer **2 (a)** and the emission spectra of the dendrimer and its different components **2 (b)**.[40]

Although single molecule or dendrimer based energy transfer is useful in light harvesting, these are not the kind of systems found in natural photosynthetic systems. In photosystems the complex molecules are arranged into ordered assemblies via non-covalent interactions. Thus the self-assembly of multichromophoric systems is always desired. In this regard, Wasielewski's group has come up with some novel molecules. They have synthesised a perylene diimide and pyromellitimide based architectures (Figure 1.4).[43] These molecules assemble in toluene and 2-methyltetrahydrofuran into dimers, which was confirmed by small angle x-ray scattering (SAXS) and ^{1}H-NMR measurements. These also assemble on hydrophobic surfaces giving rod shaped morphology of around 130 nm. The photophysical study shows that the singlet-singlet annihilation occurs on the time scale of natural photosynthetic systems. The same group has also shown the self-assembly of multichromophoric systems in organic solvents using phthalocyanine, porphyrins and perylene diimide as the building blocks of the multichromophore.[44,45,46]

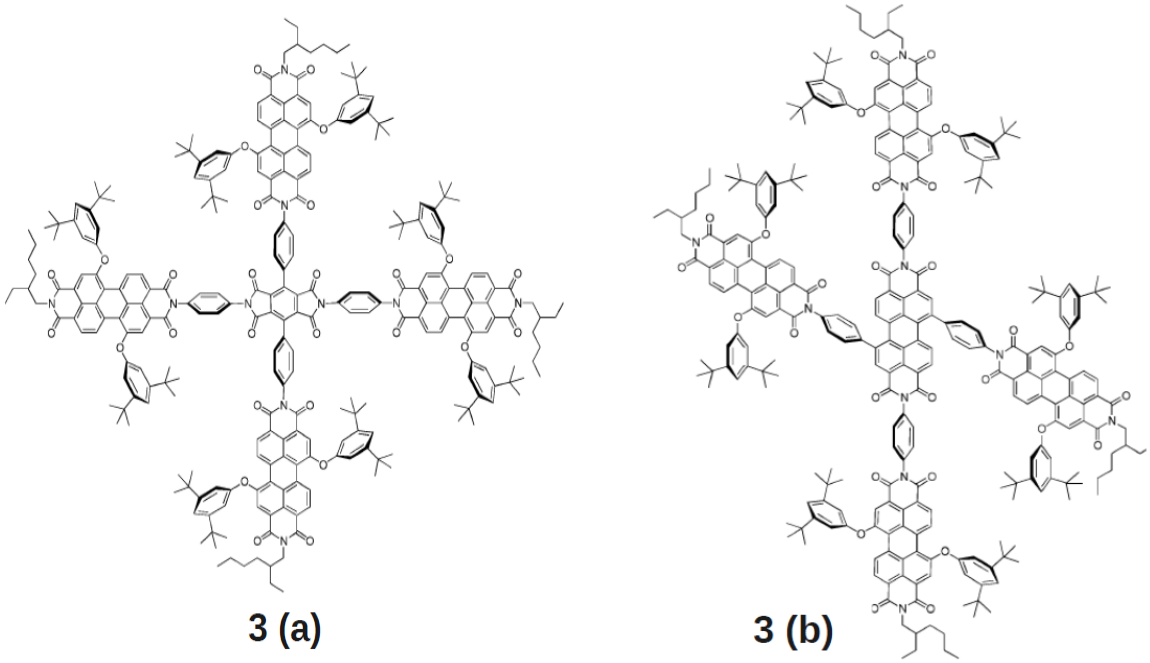

Figure 1.4. Structures of different self-assembled multichromophoric systems studied.[43]

The above example involved only smaller aggregates. But to employ these assemblies in practical applications long range assemblies are needed. Thus in order to obtain larger aggregates well defined Zn-porphyrin core was used by Wasielewski's group.[47] Here four perylene-3,4:9,10 bisimides are attached to zinc-tetraphenyl porphyrin resulting in a C_4 symmetric molecule (Figure 1.5). This molecule self-assembles both in solution and on surfaces forming nanoparticles. Apart from the antenna effect of energy transfer seen in the above cases, here rapid charge separation is also found within the nanoparticles. This latter property can be used to construct photovoltaic devices. For the efficient performance of these devices the morphology of the active layer is a critical paramter.

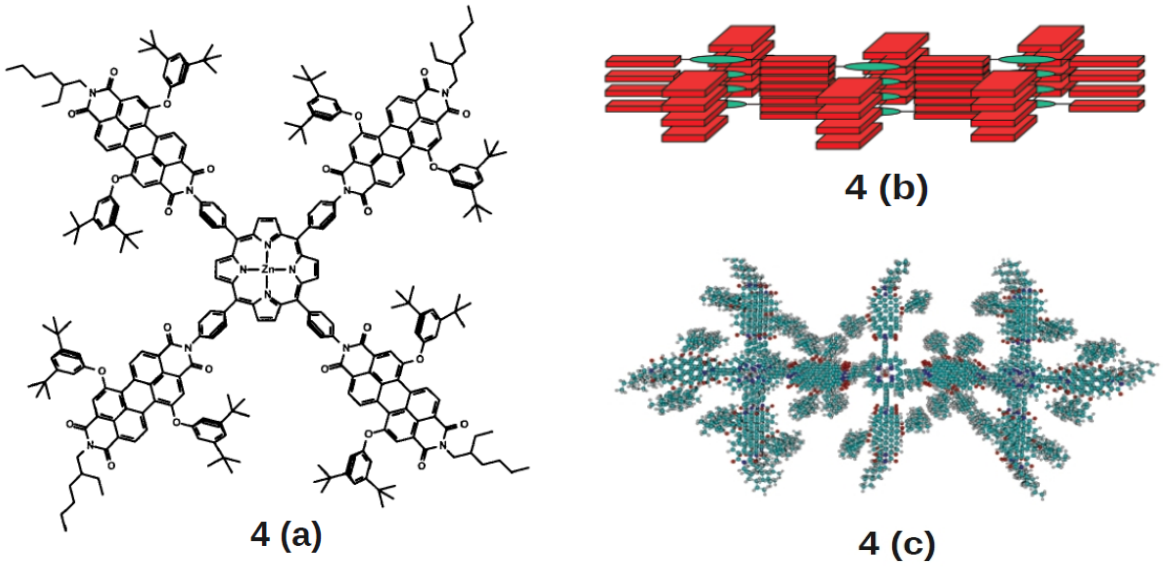

Figure 1.5. Structure of Zn-TPP-PDI_4 (**4 (a)**). Schematic of the aggregation of Zn-TPP-PDI_4 (**4 (b)**). Top view of energy minimized aggregate (**4 (c)**).[47]

The vectorial or directional energy transfer from the dendrimer or multichromophoric system we saw in the earlier examples is directed towards a central molecule. This constitutes the antenna part of the photosynthetic system. The other important part is the reaction center in which charge separation occurs in photosystems.[48,49] These generally consists of Donor-Acceptor arrays having excellent charge separation followed by oxidation or reduction processes.[50]

For this purpose of charge separation, which can be used effectively in photovoltaic devices, synthetic Donor-Acceptor (DA) dyads and triads are studied. A wide variety of DA dyads and triads are studied in literature from both experimental as well as theoretical point of view including those of fullerenes, porphyrins and carotenoids.[51,52,53] Generally these synthetic systems are used as model systems to study the different photophysical processes.

To mimic these photophysical processes one has to construct devices out of synthetic systems and study their performance. The conventional mixing of donor and acceptor has resulted in poor efficiency of the solar cells, this is mainly because of the small interfacial area of donor and acceptor and phase segregation of the two components. This problem is not only for solar cells but also for Field Effect Transistors (FET). To overcome these problems, self-assembly of functional molecules is a potent approach. Through this self-assembly approach we can create ordered channels of donor and acceptor arrays which have better interfacial area and they also help in better charge transport. Many techniques of self-assembly like self-sorting or orthogonal assembly[54] and liquid crystalline mesophases[55] are used to improve the device performance. The liquid crystalline approach has shown some reasonable promise in terms of device performance. And the approach of orthogonal self-assembly has gained more importance in the last few years and thus the concept will be explained below.

An orthogonal self-assembly approach involves individual stacks of donor and acceptor molecules arranged in a common solvent, they can even be attached through non-covalent interactions like hydrogen bonding. Figure 1.6 shows a schematic of such an orthogonal self-assembly of donors and acceptors.

Figure 1.6 Schematic of orthogonal self-assembly.

Such an orthogonal approach was used by Meijer and coworker in which a perylene bisimide substituted with aromatic gallic wedges, chiral aliphatic chains and ethylene oxides was used as an n-type material and oligo-(phenylenevinylene) (OPV) bearing hydrogen bonding ureidopyrimidinone as p-type material (Figure 1.7).[56] Both of them individually form stacks in apolar solvents (OPV forms dimers which further assemble into extended stacks) and a 1:1 mixture in apolar solvent like methylcyclohexane result in orthogonal stacks, this was proved by different spectroscopic techniques like UV/Vis, Circular dichroism and fluorescence. These orthogonal stacks were dropcasted and their photovoltaic activity was checked. These aggregates did not show good solar cell performance, possibly because of the lateral arrangement of stacks rather than the prefered vertical arrangement. In an another report from the same group, it was observed that without the ordering of chromophores through non-covalent interactions, the device performance falls off. But using hydrogen bonding between the donor and acceptor helps to arrange them into orthogonal stacks leading to ambipolar charge transport property.[57]

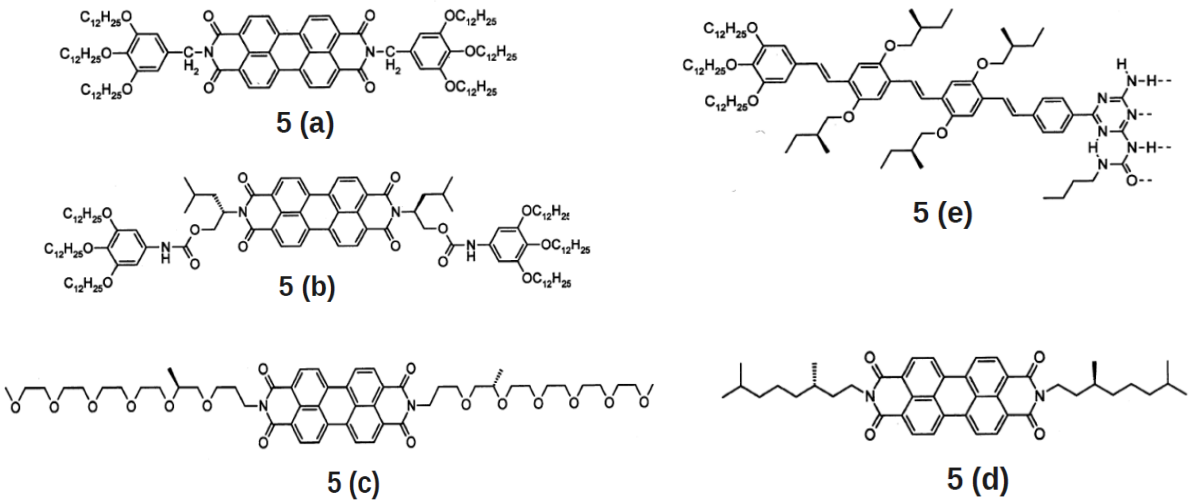

Figure 1.7 Different chromophores used in orthogonal self-assembly. Perylenebisimides (**5 (a)** to **5 (d)**) and OPV (**5 (e)**).[56]

Most of the work involving the self-assembly of these Donor and Acceptor systems consists of perylenebisimide as the acceptor and other donors.[58,59,60,61,62] This is due to the well known aggregation behaviour of perylene dyes. Other better acceptors such as fullerenes are not extensively used because the self-assembly process is hindered as a result of the bulky nature of fullerene. The Donor and Acceptor can be covalently linked or can be connected through non-covalent interaction like hydrogen bonding.

1.5 Aim of the thesis

Having seen the importance of self-assembled multichromophoric systems in artifical photosynthesis and Donor-Acceptor systems, here we try to construct such systems based on a new chromophore namely coronene. A new type of electron acceptor molecule is envisaged, namely coronenetetraimide. The synthetic aspects of this molecule will be the content of chapter 2. Also a new Donor-Acceptor-Donor molecule consisting of coronene bisimide as the electron acceptor is studied. The self-assembly aspects of this molecule are studied in chapter 3. Thus in a way this thesis deals mainly with the chemistry of coronene imides leading to newer and more novel derivatives and their self-assembly.

1.6 References

1. Pedersen, C. J. *J. Am. Chem. Soc.* **1967**, *89*, 7017.
2. Adams, R.; Whitehill, L. N. *J. Am. Chem. Soc.* **1941**, *63*, 2073.
3. Lehn, J. M. *Supramolecular Chemistry*; Wiley-VCH: Weinheim, Germany, **1995**.
4. Prins, L. J.; Reinhoudt, D. N.; Timmerman, P. *Angew. Chem. Int. Ed.* **2001**, *40*, 2382.
5. Würthner, F.; Meerholz, K. *Chem. Eur. J*. **2010**, *16*, 9366.
6. Müller-Dethlefs, K.; Hobza, P. *Chem. Rev.* **2000**, *100*, 143.
7. Steed, J. W.; Atwood, J. L. *Supramolecular Chemistry*, Wiley-VCH, Weinheim, **2000**.
8. González-Rodriguez, D.; Schenning, A. P. H. J. *Chem. Mater.* **2011**, *23*, 310.
9. El-ghayoury, A.; Schenning, A. P. H. J.; van Hal, P. A.; van Duren, J. K. J.; Janssen, R. A. J.; Meijer, E. W. *Angew. Chem. Int. Ed*. **2001**, *40*, 3660.
10. El-ghayoury, A.; Peeters, E.; Schenning, A. P. H. J.; Meijer, E. W. *Chem. Commun.* **2000**, 1969.
11. Kaiser, T. E.; Stepanenko, V.; Würthner, F. *J. Am. Chem. Soc.* **2009**, *131*, 6719.
12. Locklin, J.; Youk, J. H.; Xia, C.; Park, M.-K.; Fan, X. Advincula, R. C. *Langmuir* **2002**, *18*, 877.
13. Arnaud, A.; Belleney, J.; Boué, F.; Bouteiller, L.; Carrot, G.; Wintgens, V. *Angew. Chem. Int. Ed.* **2004**, *43*, 1718.
14. Ruan, Y.-B.; Li, A.-F.; Zhao, J.-S.; Shen, J.-S.; Jiang, Y.-B. *Chem. Commun.* **2010**, *46*, 4938.
15. Wasielewski, M. R. *Chem. Rev.* **1992**, *92*, 435.
16. Lavie-Cambot, A.; Lincheneau, C.; Cantuel, M.; Leydet, Y.; McClenaghan, N. D. *Chem. Soc. Rev.* **2010**, *39*, 506.

17. Adronov, A.; Gilat, S. L.; Fréchet, J. M. J.; Ohta, K.; Neuwahl, F. V. R.; Fleming, G. R. *J. Am. Chem. Soc.* **2000**, *122*, 1175.
18. Schenning, A. P. H. J.; Jonkheijm, P.; Hoeben, F. J. M.; van Herrikhuyzen, J.; Meskers, S. C. J.; Meijer, E. W.; Herz, L. M.; Daniel, C.; Silva, C.; Phillips, R. T.; Friend, R. H., Beljonne, D.; Miura, A.; De Feyters, S.; Zdanowska, M.; Uji-i, H.; De Schryver, F. C.; Chen, Z.; Würthner, F.; Mas-Torrent, M.; den Boer, D. Durkut, M.; Hadley, P. *Synt. Met.* **2004**, *147*, 43.
19. Hoeben, F. J. M.; Jonkheijm, P.; Meijer, E. W.; Schenning, A. P. H. J. *Chem. Rev.* **2005**, *105*, 1491.
20. Tinnefeld, P.; Hofkens, J.; Herten, D. P.; Masuo, S.; Vosch, T.; Cotlet, M.; Habuchi, S.; Müllen, K.; De Schryver, F. C.; Sauer, M. *Chem. Phys. Chem.* **2004**, *5*, 1786.
21. Schroeyers, W.; Vallée, R.; Patra, D.; Hofkens, J.; Habuchi, S.; Vosch, T.; Cotlet, M.; Müllen, K.; Enderlein, J.; De Schryver, F. C. *J. Am. Chem. Soc*. **2004**, *126*, 14310.
22. De Schryver, F. C.; Vosch, T.; Cotlet, M.; van der Auweraer, M.; Müllen, K.; Hofkens, J. *Acc. Chem. Res.* **2005**, *38*, 514.
23. Métivier, R.; Kulzer, F.; Weil, T.; Müllen, K.; Basché, T. *J. Am. Chem. Soc*. **2004**, *126*, 14364.
24. Palermo, V.; Schwartz, E.; Liscio, A.; Otten, M. B. J.; Müllen, K.; Nolte, R. J. M.; Rowan, A. E.; Samori, P. *Soft Matter* **2009**, *5*, 4680.
25. Flors, C.; Oesterling, I. Schnitzler, T.; Fron, E.; Schweitzer, G.; Silwa, M.; Hermann, A.; van der Schryver, F.; Müllen, K.; Hofkens, J. *J. Phys. Chem. C*. **2007**, *111*, 4861.
26. Oesterling, I.; Müllen, K. *J. Am. Chem. Soc.* **2007**, *129*, 4595.
27. Chrisstoffels, L. A. J.; Adronov, A.; Fréchet, J. M. J. *Angew. Chem. Int. Ed*. **2000**, *39*, 2163.
28. Brousmiche, D. W.; Serin, J. M.; Fréchet, J. M. J. *J. Phys. Chem. B*. **2004**, *108*, 8592.

29. Furuta, P.; Brooks, J.; Thompson, M. E.; Fréchet, J. M. J. *J. Am. Chem. Soc*. **2003**, *125*, 13165.

30. Brousmiche, D. W.; Serin, J. M.; Fréchet, J. M. J.; He, G. S.; Lin, T.-C.; Chung, S.-J.; Prasad, P. N.; Kannan, R.; Tan, L.-S. *J. Phys. Chem. B*. **2004**, *108*, 8592.

31. Wasielewski, M. R. *J. Org. Chem*. **2006**, *71*, 5051.

32. Wasielewski, M. R. *Acc. Chem. Res*. **2009**, *42*, 1910.

33. Harriman, A.; Mallon, L.; Ziessel, R. *Chem. Eur. J.* **2008**, *14*, 11461.

34. Stéphane, D.; Ziessel, R. *Tetrahedron Lett.* **2009**, *50*, 1203.

35. Albert-Seifried, A.; Finlayson, C. E.; Laquai, F.; Friend, R. H.; Sawger, T. M.; Kouwer, P. H. J.; Juricek, M.; Kitto, H. J.; Valeter, S.; Nolte, R. J. M.; Rowan, E. A. *Chem. Eur. J*. **2010**, *16*, 10021.

36. Terenziani, F.; Mongin, O.; Katan, C.;Bhatthula, B. K. G.; Blanchard-Desce, M. *Chem. Eur. J.* **2006**, *12*, 3089.

37. Valeur, B.; Laray, I. *Inorg. Chim. Acta*, **2007**, *360*, 765.

38. Souchon, V.; Leray, I.; Berberan-Santos, M. N.; Valeur, B. *Dalton Trans*. **2009**, 3988.

39. Banerji, N.; Furstenberg, A.; Bhosale, S.; Sisson, A. L.; Sakai, N.; Matile, S.; Vauthey, E. *J. Phys. Chem. B*. **2008**, *112*, 8912.

40. Dichtel, W. R.; Hecht, S.; Fréchet, J. M. J. *Org. Lett*. **2005**, *7*, 4451.

41. Serin, J. M.; Brousmiche, D. W.; Fréchet, J. M. J. *Chem. Commun*. **2002**, 2605.

42. Cotlet, M.; Vosch, T.; Habuchi, S.; Weil, T.; Müllen, K.; Hofkens, J.; De Schryver, F. *J. Am. Chem. Soc*. **2005**, *127*, 9760.

43. Ahrens, M. J.; Sinks, L. E.; Rybtchinski, B.; Liu, W.; Jones, B. A.; Giamio, J. M.; Goshe, A. J.; Tiede, D. M.; Wasielewski, M. R. *J. Am. Chem. Soc*. **2004**, *126*, 8284.

44. Li, X.; Sinks, L. E.; Rybtchinski, B.; Wasielewski, M. R. *J. Am. Chem. Soc*. **2004**, *126*, 10810.

45. Rybychinski, B.; Sinks, L. E.; Wasielewski, M. R. *J. Am. Chem. Soc*. **2004**, *126*, 12268.

46. Kelley, R. F.; Shin, W. S.; Rybtchinski, B.; Sinks, L. E.; Wasielewski, M. R. *J. Am. Chem. Soc*. **2007**, *129*, 3173.

47. van der Boom, T.; Hayes, R. T.; Zhao, Y.; Bushard, P. J.; Weiss, E. A.; Wasielewski, M. R. *J. Am. Chem. Soc*. **2002**, *124*, 9582.

48. Ivashin, N.; Källebring, B.; Larsson, S.; Hansson, Ö. *J. Phys. Chem. B*. **1998**, *102*, 5017.

49. Haffa, A. L. M.; Lin, S.; Williams, J. C.; Bowen, B. P.; Taguchi, A. K. W.; Allen, J. P.; Woodbury, N. W. *J. Phys. Chem. B*. **2004**, *108*, 4.

50. Imahorei, H.; Tamaki, K.; Guldi, D. M.; Luo, C.; Fujitsuka, M.; Ito, O.; Sakata, Y.; Fukuzumi, S. *J. Am. Chem. Soc*. **2001**, *123*, 2607.

51. Guldi, D. M. *Chem. Soc. Rev*. **2002**, *31*, 22.

52. Spallanzani, N.; Rozzi, C. A.; Varsano, D.; Baruah, T.; Pederson, M. R.; Manghi, F.; Rubio, A. *J. Phys. Chem. B*. **2009**, *113*, 5345.

53. Mativetsky, J. M.; Kastler, M.; Savage, R. C.; Gentilini, D.; Palma, M.; Pisula, W.; Müllen, K.; Samon, P. *Adv. Funct. Mater*. **2009**, *19*, 2486.

54. Pal, A.; Karthikeyan, S.; Sijbesma, R. P. *J. Am. Chem. Soc*. **2010**, *132*, 7842.

55. Schmidt-Mende, L.; Fechtenkotter, A.; Müllen, K.; Moons, E.; Friend, R. H.; Mackenzie, J. D. *Science* **2001**, *293*, 1119.

56. van Herrikhuyzen, J.; Syamakumari, A.; Schenning, A. P. H. J.; Meijer, E. W. *J. Am. Chem. Soc*. **2004**, *126*, 10021.

57. Jonkheijm, P.; Stutzmann, N.; Chen, Z.; de Leeuw, D. M.; Meijer, E. W.; Schenning, A. P. H. J.; Würthner, F. *J. Am. Chem. Soc*. **2006**, *128*, 9535.

58. Syamakumari, A.; Schenning, A. P. H. J.; Meijer, E. W. *Chem. Eur. J.* **2002**, *8*, 3353.

59. Beckers, E. H. A.; Meskers, S. C. J.; Schenning, A. P. H. J.; Chen, Z.; Würthner, F.; Janssen, R. A. J. *J. Phys. Chem. A.* **2004**, *108*, 6933.

60. Beckers, E. H. A.; Meskers, S. C. J.; Schenning, A. P. H. J.; Chen, Z.; Würthner, F.; Marsal, P.; Beljonne, D.; Cornil, J.; Janssen, R. A. J. *J. Am. Chem. Soc*. **2006**, *128*, 649.

61. Peeters, E.; van Hal, P. A.; Meskers. S. C. J.; Janssen, R. A. J.; Meijer, E. W. *Chem. Eur. J.* **2002**, *8*, 4470.

62. Beckers, E. H. A.; Chen, Z.; Meskers, S. C. J.; Jonkheijm, P.; Schenning, A. P. H. J.; Li, X.-Q.; Osswald, P.; Würthner, F.; Janssen, R. A. J. *J. Phys. Chem. B.* **2006**, *110*, 16967.

Chapter 2

Towards the synthesis of Coronenetetraimide derivatives

Abstract

As the quest for more efficient photovoltaic materials increases, new materials with good electronic and self-assembly properties are sought-after in molecular electronics. In the wake of this, here we present the synthesis of a new four fold symmetric coronenetetraimide, which is capable of acting as an efficient electron acceptor. We take advantage of the microwave reaction to perform Diels-Alder reactions to increase the yield of the synthesis.

2.1 Introduction

Coronene is the smallest homologue of benzene possessing a six fold symmetry. Because of the presence of a perfect delocalisation of the electron density over the entire molecule it is chemically very stable. In the crystalline state, the molecules are stacked parallel to one another in a cofacial manner with a intermolecular distance of 3.43 Å, which is considerably smaller compared to other aromatic systems. This very short intermolecular distance results in the very good overlap of wavefunctions of the molecules adjacent to each other leading to better transport properties.[1,2]

Coronene derivatives have been exploited as liquid crystalline materials[3,4,5] and also some of the benzoperylene ester derivatives have been shown to be electroluminescent.[6] Some of the simplest accessible derivatives of coronene are coronene diimides (CDI) in which the imide is a part of a six membered ring (Figure 2.1 **CDI(A)**). They are synthesised from perylene bisimides by bromination followed by a sonogashira coupling and then the cyclisation leading to coronene bisimides.[7,8,9] Most of the coronene bisimide derivatives follow the procedure described above leading to different derivatives. Recently, another type of coronene diimides was synthesised in which the imide forms the part of a five membered ring (Figure 2.1 **CDI (B)**).[10] Also a new class of three fold symmetric derivatives of coronene leading to some of the interesting tetrathiafulvalene fused coronene derivatives was studied.[11,12,13] Heteroatom containing coronenes are also known.[14]

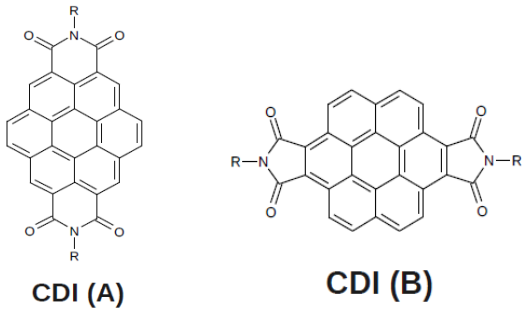

Figure 2.1 Two different types of coronene dimides.

The synthesis of these macrocyclic aromatic hydrocarbons has a long history starting from Clar, Scholl and coworkers with the recent contributions from Klaus müllen's group.[15,16,17,18] The synthesis has many approaches, among them the most important ones will be discussed below. In the first approach the precursors like polyphenylenes of the macrocycle are built and then oxidative cyclodehydrogenation is carried out leading to the desired product.[19,20] The size of the desired product can be well controlled in this method. But generally this method has been applied to only large enough hydrocarbons and it is futile for medium or smaller hydrocarbons. In the second approach which is suitable for smaller or medium hydrocarbons, these are built by brute force techniques from some smaller analogues mainly using Diels-Alder reaction.[9] These smaller building units can be perylene or other polycyclic arylenes. These have two regions namely peri region and bay region in the structures (Figure 2.2).

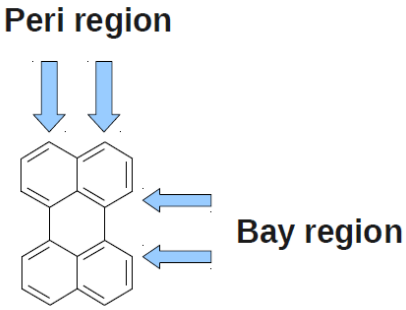

Figure 2.2 Structure of perylene showing its different regions.

The Diels-Alder reaction of the perylenes takes place in the bay region to undergo core expansion leading to higher hydrocarbons. But the Diels-Alder reaction in the bay region of perylene is difficult and requires harsh conditions. Other molecules like phenanthrene and triphenylene have very low reactivity in the bay region and often they do not undergo reaction even in harsher conditions.[21] This is because of the very high energetic cost to be paid to break the aromaticity in the molecule leading to a hydrogenated Diels-Alder adduct. But as we move to higher hydrocarbons like tetrabenzopyrene and tetrabenzocoronene this tendency of reduced reactivity decreases, leading to enhanced propensity of the bay region Diels-Alder reaction.[22]

This approach of Diels-Alder reaction was used to come up with a new way of synthesis for a whole range of perylene, benzoperylene and coronene derivatives.[23,24] The approach involved the use of two fold benzogenic Diels-Alder reaction on perylene or perylene derivatives under harsher reaction conditions to yield coronene derivatives. The sailent features of this method are, the use of esters of anhydride as precursors for Diels-Alder reaction and a two-fold benzogenic Diels-Alder reaction. The first Diels-Alder reaction on perylene derivatives proceeds with moderate yield using not so harsh reaction conditions. But the second Diels-Alder reaction on the benzoperylene is difficult, thus ending up in moderate to low yields. Thus achieving second Diels-Alder reaction is a challenge.

In the present work we address this issue of decreased Diels-Alder reactivity by using microwave approach. To further increase the yield of the reaction, another approach using esterification is provided. Using this as a building block many new electron acceptor chromophores can be built as shown below.

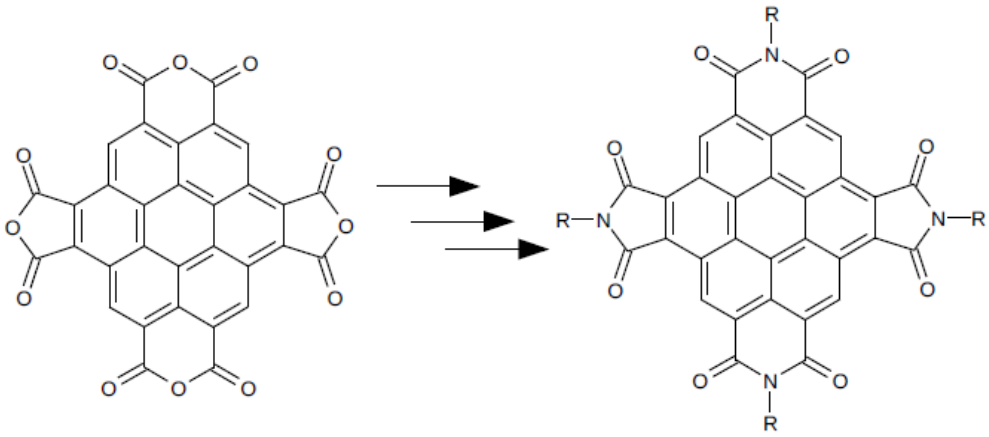

2.2 Our approach to the problem

Here we start with perylene dianhydride and perform an esterification to obtain the tetraisobutyl ester of perylene dianhydride (PDI) (scheme 1). This esterification step is needed to convert PDI into a better diene. Because perylene as such is less reactive in the bay region and in case of PDI two very strong electron withdrawing groups such as anhydrides are present, thus reducing the propensity of the PDI as a diene. After this is the very crucial step of Diels-Alder reaction. The Alibert-Fouet et al. group[24] performed this step using of N-ethylmaleimide as the dienophile, p-chloranil as a reagent for oxidative cylcodehydrogenation, p-hydroxy anisole to prevent the polymerisation of N-ethylmaleimide at 240 ^{0}C for 36 hours. At such an elevated temperature, N-ethylmaleimide itself acts as the solvent by melting. This reaction generally leads to low yields and a lot of charry products. Thus a new method had to be designed to circumvent this problem.

We tried the reaction with nitrobenzene as solvent and other components, perylene tetraester (2), N-ethylmaleimide, p-hydroxy anisole and p-chloranil under inert conditions for different times ranging from 18 hours to 96 hours at 240 ^{0}C. The ^{1}H-NMR analysis of the crude product showed the presence of benzoperylene adduct (mono adduct) as well as coronene adduct (di adduct). But the benzoperylene adduct turned out to be the major one with a small fraction of the desired coronene adduct i,e a 3:1 product was obtained in favour of mono adduct to di adduct respectively. This is understandable because once the mono adduct forms the molecule becomes a weaker diene because of the electron withdrawing nature of the added imide group on the molecule. Thus the next step will be highly unfavourable. To overcome this we used a microwave technique in which we were able to improve a lot on the ratio of mono to di product (mono to di ratio 2:1), although we were not able to completely convert it into the di product. Microwave reaction helps over other thermal reactions, because it not only provides the temperature but also the required

confinement and the high pressure for the reaction to occur. This idea is also supported by the work of M. Fujita and coworkers on the Diels-Alder reactions of unreactive species like napthalene and triphenylene in molecular flasks.[25,26,27] We are currently exploring the possibilities of using the mono adduct to convert into the di adduct using esterification followed by Diels-Alder reaction.

2.3 Synthetic scheme

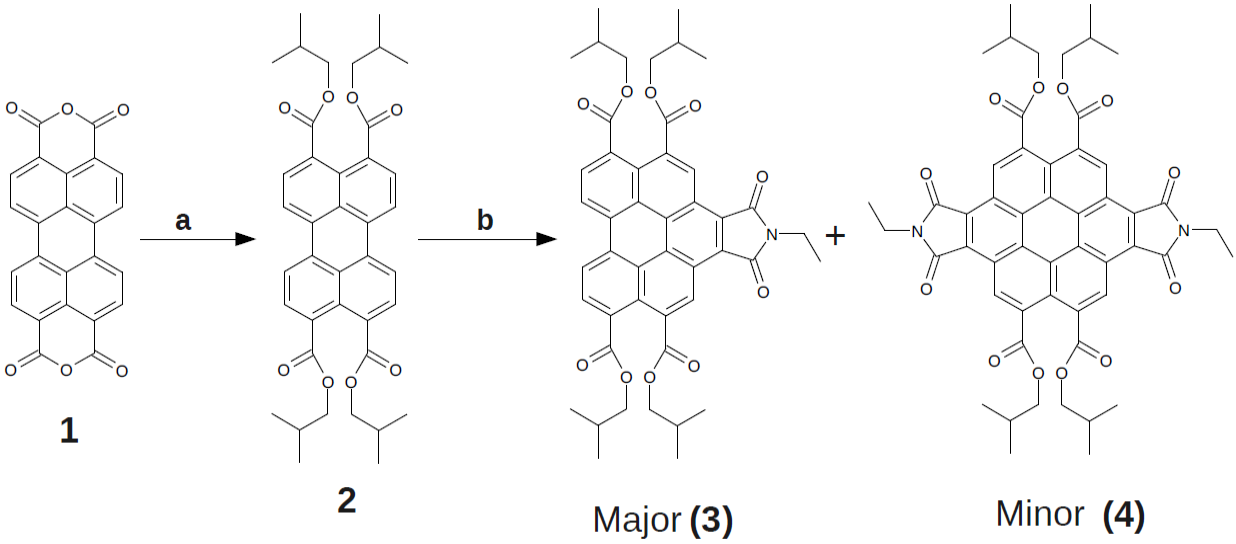

Scheme 1. (a) Isobutanol, 1-bromo-2-methyl propane, DBU, Acetonitrile, 95 ^{0}C reflux (b) Microwave 600 W, N-ethylmaleimide, Nitrobenzene 1 h.

First we start with the esterification of perylene-3,4:9,10:dianhydride (**1**) using 1,8-Diazabicycloundec-7-ene (DBU) as non-nucleophilic base with isobutanol as the precursor of the ester. This proceeds smoothly with a good yield of around 80 %. The next step involves the Diels-Alder reaction of this perylene tetraester (**2**). As described earlier the thermal reaction turned out to be futile. So microwave reaction was performed using nitrobenzene and N-ethylmaleimide as the reagents (Scheme 1). Different parameters like duration of the reaction time, power of the microwave and the time for which it should be allowed to cool once the reaction is done and so on were optimised for the reaction. The summary is given in Table 2.1. From Table 2.1 we can see that N-ethylmaleimide is a better dienophile when compared to maleic anhydried under given reaction

conditions although the former is more sensitive to reaction conditions. Here nitrobenzene has a dual role, both as a solvent and also as an oxidising agent to effect the cyclodehydrogenation leading to the aromatisation.

Dienophiles used	Microwave power	Reaction duration	Comment
N-ethylmaleimide	600 W	1 hour	Both **3** and **4** in the ratio of 2 : 1
	600 W	2 hours	Both **3** and **4** in the ratio of 2 : 1
	800 W	1 hour	A dark brown to balck product was obtained
	900 W	1 hour	A completely charred product obtained
Maleic anhydride	600 W	1 hour	Only starting material
	800 W	1 hour	Only **3** and starting material is obtained
	900 W	1 hour	Major of **3** and small portion of **4** is obtained

Table 2.1 Different reaction condtions and reagents used to optimize the microwave reaction.

The crude product showed a ratio of 2:1 for the formation of **3** and **4** respectively. Initial few silica gel column chromatography was done to separate impurities other than **3** and **4**. As it turned out the two spots of products **3** and **4** were very close in thin layer chromatography (TLC), within a retention factor (Rf) of 0.1. Many atttempts to separate the two components using different stationary and mobile phases failed. Neutral alumina showed some promise in Thin Layer Chromatography but the components did not separate in a column chromatography. Size exclusion chromatography also could not be used because of the similar hydrodynamic radius of both molecules and a small difference in mass.

Only once with a silica gel column which was run for a long time, we could separate the components. The amount of **3** was more compared to **4** as expected. So in order to enhance the

yield of the reaction, **3** was hydrolysed followed by dehydration leading to **6**. A smiliar esterification was performed on **6** to obtain the hexaester derivative of benzoperylene **7** (Scheme 2). This step was followed to increase the reactivity of **3** by transforming it into a better diene.

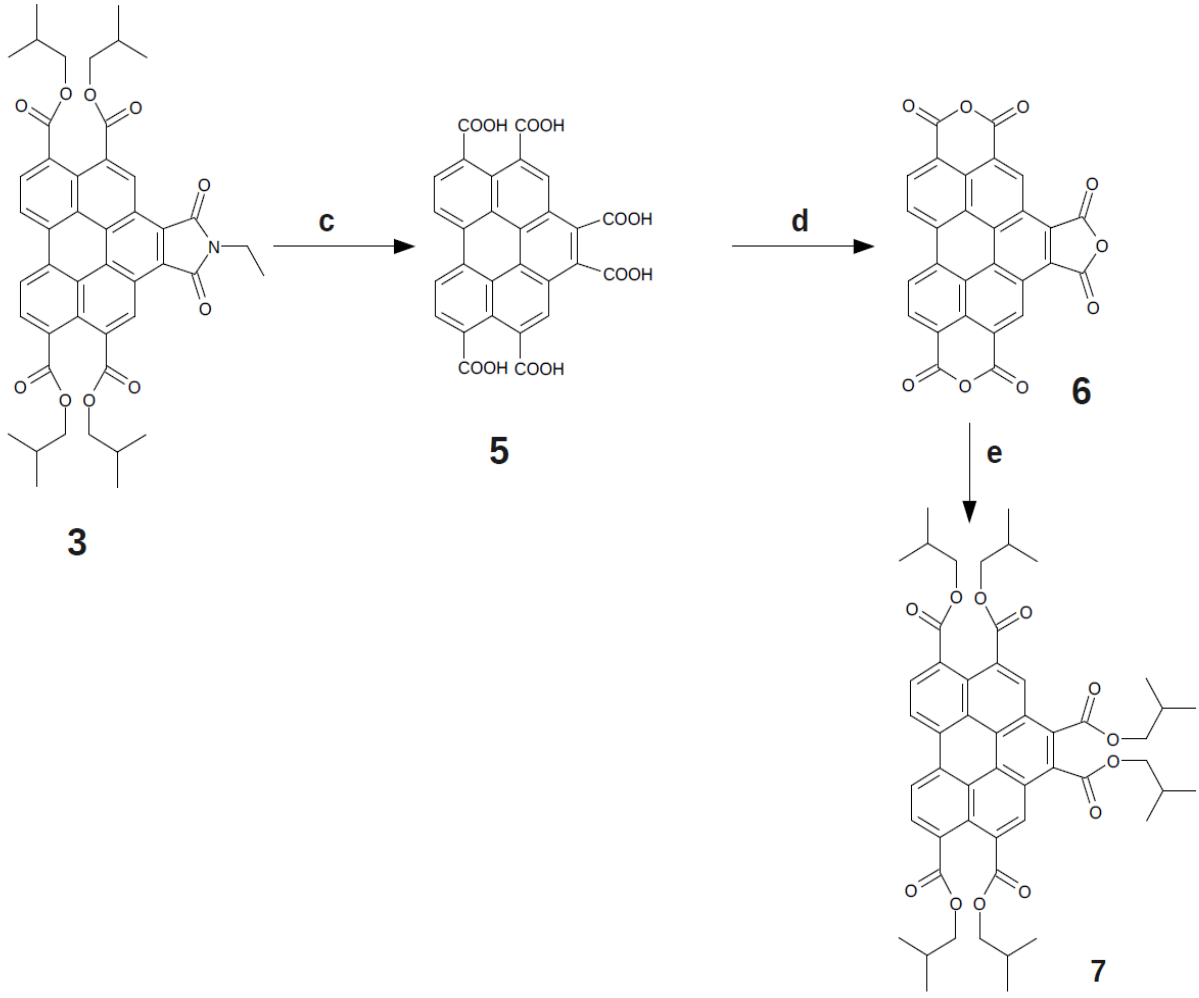

Scheme 2. (c) KOH, MeOH, K_2CO_3, heat, HCl (d) Heat at 120 ^{0}C for 24 h (e) Isobutanol, 1-bromo-2-methyl propane, DBU, Acetonitrile, 95 ^{0}C reflux

2.4 Conclusions and future work

Thus we have developed a synthetically easy, high yielding protocol towards the synthesis of more electron deficient coronenetetraimide by using microwave technique. We believe that this technique can be applied to other Diels-Alder reactions which require harsh conditions and

lengthy reaction times to ease the process of synthesis. We further look forward to carrying out the Diels-Alder reaction on **7** to yield **8**, and also the separation of **3** and **4** using chromatographic techniques like chromatotron and recycling gel permeation chromatography. The future reaction schemes are shown in scheme 3.

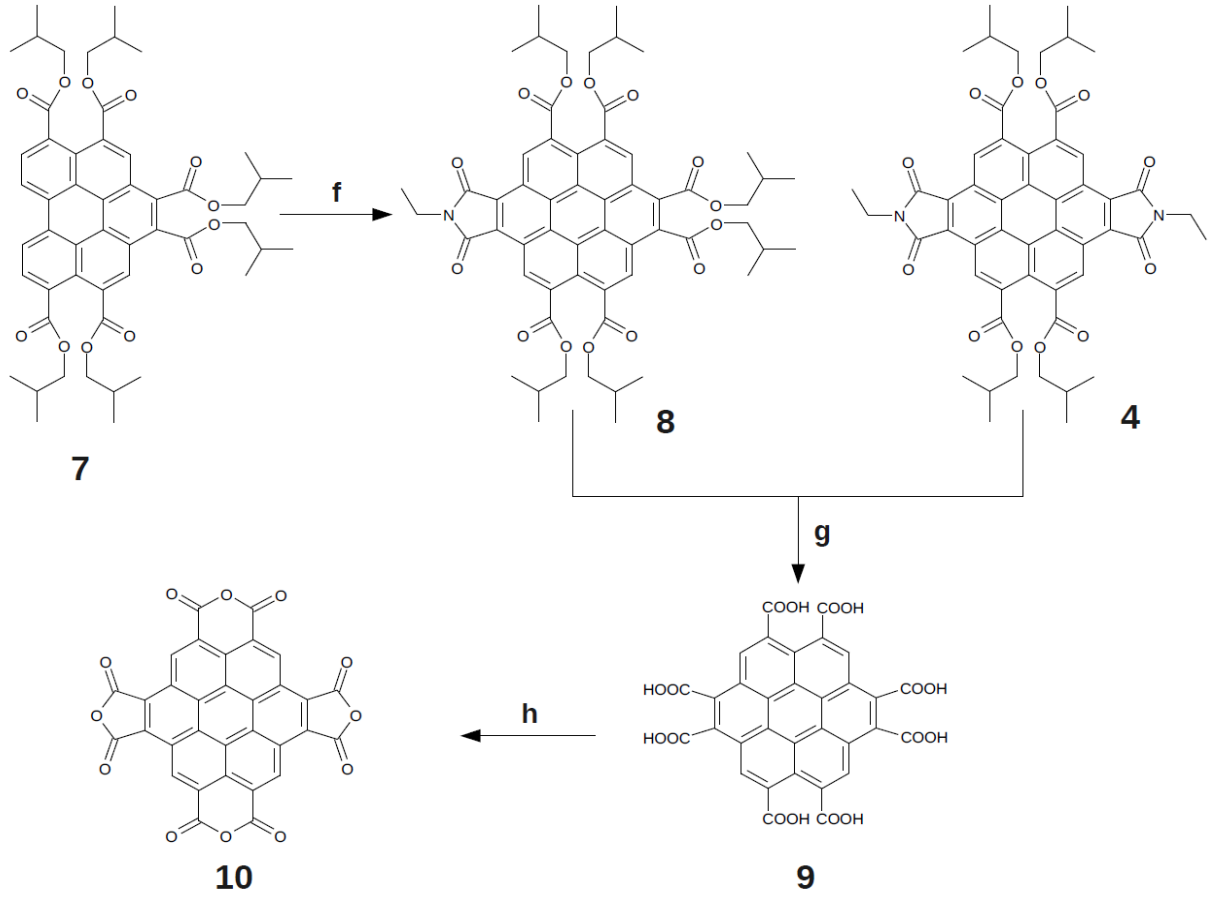

Scheme 3. (f) Microwave 600 W, N-ethylmaleimide, Nitrobenzene, 1 h (g) KOH, MeOH, K_2CO_3, heat, HCl (h) Heat at 120 ^{0}C for 24 h.

Using this new electron acceptor as a core we envisage to make a variety of new self-assembling multichromophoric systems and study their applications in photovoltaic devices. The schematic showing the possible self-assembly of multichromphoric systems involving coronenetetraimide as an acceptor and others donors is given below (Figure 2.3).

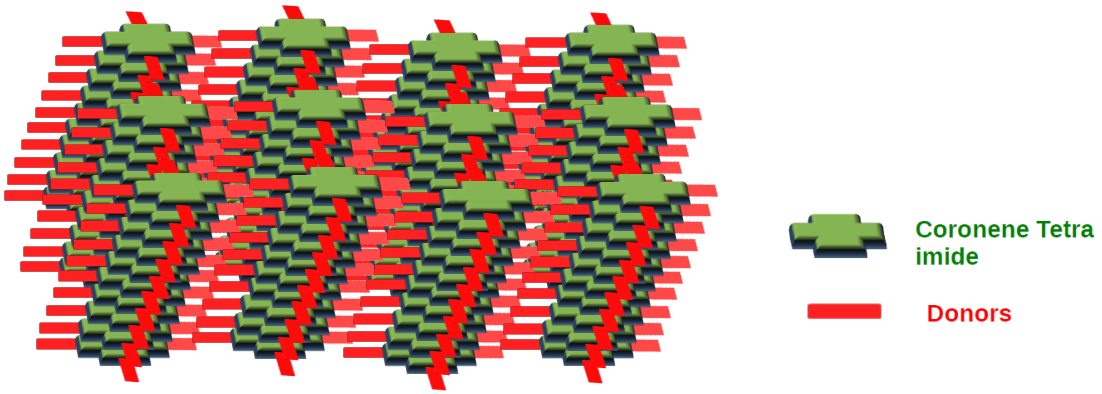

Figure 2.3 Schematic showing the possible self-assembly of coronenetetraimide based multichromophore.

2.5 Experimental section

General Methods

NMR Measurements: NMR spectra were obtained with a Brucker AVANCE 400 (400 MHz) Fourier transform NMR spectrometer with chemical shifts reported in parts per million (ppm) with respect to Tetramethylsilane (TMS).

Matrix-assisted laser desorption ionization time-of-flight (MALDI-TOF): MALDI-TOF spectra were obtained on a Brucker ultraflex 2 MALDI-TOF mass spectrometer with α-cyano-4-hydroxycinnamic acid matrix.

Synthesis of **2**

1 (10 g, 25.49 mmol), 1-bromo-2-methyl-propane (50 g, 674.5 mmol), Isobutanol (32.5 g, 438.4 mmol), DBU (37.5 g, 246.3 mmol) and 400 mL of acetonitrile were taken in a three necked 1000 mL Round Bottom Flask (RBF) connected to a condenser and fitted with a magnetic stirrer. The mixture turned to an orange precipitate even before stirring. The mixture is refluxed at 95 ^{0}C for 12 hours. Then the reaction mixture was allowed to cool down to

room temperature. The precipitation of the orange solid was completed by the addition of 400 mL of methanol while stirrring. The precipitate was filtered off under suction to yield an orange colored solid. It was then dried in vacuum oven at 75 ^{0}C to remove the traces of methanol. The crude product was purified by a silica gel column chromatography (100–200 mesh size) using chloroform as the eluent. The second fraction was the desired product. Orange solid, 13.95 g (yield 84 %). ^{1}H-NMR (400 MHz, $CDCl_3$): δ ppm 8.26 (d, *J*=8 Hz, 4H, Ar-H), 8.03 (d, *J*=8 Hz, 4H, Ar-H), 4.11 (d, *J*=6.8 Hz, 8H, OCH_2), 2.10 (m, 4H, CH), 1.04 (d, *J*=6.8 Hz, 24H, CH_3); MALDI-TOF MS m/z 653 $[M+H]^+$ Cacld for $C_{40}H_{44}O_8$ 652.

Synthesis of **3** and **4**

2 (500 mg, 0.765 mmol), N-ethylmaleimide (1.531 g, 12.24 mmol) and 10 mL of nitrobenzene were taken in a clean teflon microwave autoclave. The autoclave was heated at 600 W for 1 hour, with a break of 2 minutes every 10 minutes of heating to avoid the possible explosion of the reaction due to excessive pressure. After the heating was over, it was allowed to cool down for about one and half hour. Then 20-30 mL of methanol was added to the warm solution to precipitate the products. This precipitation also helped to remove nitrobenzene which was miscible with methanol. The products were filtered under suction to obtain an orange solid. Then it was dired in vacuum oven at 75 ^{0}C to remove the traces of methanol. The crude product was purified by silica gel chromatography (100-200 mesh size) using chloroform as the eluent to remove all other impurities expect the mixture of **3** and **4**. This mixture was separated by a silica gel column chromatography (100-200 mesh size) which was run at a very slow pace and for a long time. **3** was an orangish-yellow product (150 mg, 26 % yield): ^{1}H-NMR (400 MHz, $CDCl_3$) δ ppm 9.69 (s, 2H, Ar-H), 8.83 (d, *J*=8.4 Hz, 2H, Ar-H), 8.37 (d, *J*=8.4 Hz, 2H, Ar-H), 4.27 (d, *J*=6.8 Hz, 4H, OCH_2), 4.22 (d, *J*=6.8 Hz, 2H, OCH_2), 2.32 (m, 2H, CH), 2.19 (m, 2H, CH), 1.46 (t, *J*=7.2 Hz, 3H, CH_3),

1.21 (d, *J*=6.4 Hz, 12H, CH_3), 1.12 (t, *J*=6.8 Hz, 12H, CH_3); MALDI-TOF MS m/z 776 $[M+H]^+$ Cacld for $C_{46}H_{49}NO_{10}$ 775. **4** was a yellow colored solid (75 mg, 11 % yield): ^{1}H-NMR (400 MHz, $CDCl_3$) δ ppm 10.62 (s, 4H, Ar-H), 4.40 (d, *J*=6.8 Hz, 8H, OCH_2), 4.10 (q, *J*=7.6 Hz, 4H, CH_2N), 2.36 (m, *J*=7.2 Hz, 4H, CH), 1.55 (t, *J*=7 Hz, 6H, CH_3), 1.22 (d, *J*=6.8 Hz, 24H, CH_3); MALDI-TOF MS m/z 895 $[M+H]^+$ Cacld for $C_{52}H_{50}N_2O_{12}$ 894.

Synthesis of **6**

3 (250 mg, 0.322 mmol), K_2CO_3 (7.5 g, 54.26 mmol) and 20 mL of methanol were taken in a 50 mL two necked RBF fitted with a reflux condenser and a stirrer. The mixture was heated at 90 ^{0}C for one hour and then the temperature was raised to 150 ^{0}C (oil bath temperature) and maintained for an additional 12 hours. After this, the reaction mixture had turned into a paste. To push the hydrolysis to completion, KOH (3.9 g, 69.511 mmol) and methanol (10 mL) was added to it. The heating was continued for another 5 hours. Once the reaction mixture cooled down to room temprature, it was diluted with double distilled (DD) water (100-125 mL) and acidified with excess conc. HCl till the pH of the solution became acidic. Thorough cooling was required to complete the process of precipitation. Then it was filtered out washed thoroughly with 400 mL of DD water under suction. A red colored gelatinous precipitate of the hexaacid (**5**) was obtained.The precipitate was heated under vacuum at 90 ^{0}C for 24 hours to obtain a dark red solid (73 mg, 46.56 % yield).

Synthesis of **7**

6 (72 mg, 0.1481 mmol), 1-bromo-2-methyl-propane (1.5 g, 20.23 mmol), Isobutanol (500 mg, 6.745 mmol), DBU (700 mg, 4.598 mmol) and acetonitrile (5 mL) were taken in a 10 mL two necked RBF connected to a condenser and a magnetic stirrer. The mixture was

refluxed at 95 ^{0}C for 12 hours under nitrogen atmosphere. Once the reaction mixture cooled down to room temperature, it was evaporated under vacuum to obtain orange colored crude product. This was purified by silica gel chromatography (100-200 mesh size) with 1:10 of methanol:chloroform to obtain the top spot as the product. Another size exclusion chromatography (Biobeads, SX-3, chloroform) was performed to remove lower molecular weight impurities to obtain an orange paste (110 mg, 84.6 % yield): ^{1}H-NMR (400 MHz, $CDCl_3$) δ ppm 9.20 (d, *J*=8.4 Hz, 2H, Ar-H), 9.05 (s, 2 H, Ar-H), 8.60 (d, *J*=8 Hz, 2H, Ar-H), 4.35 (d, *J*=6.8 Hz, 4H, OCH_2), 4.21 (d, *J*=1.6 Hz, 4Hz, OCH_2), 4.29 (d, *J*=1.6 Hz, 4H, OCH_2), 2.17 (m, 6H, CH), 1.08 (d, *J*=2 Hz, 12H, CH3), 1.07 (d, *J*=1.6 Hz, 12H, CH_3), 1.06 (d, *J*=2.8 Hz, 12H, CH_3); MALDI-TOF MS m/z 899 $[M+Na+H]^+$ Cacld for $C_{52}H_{60}O_{12}$ 876.

2.6 References

1. Matusi, A. H.; Mizuno, K.-I. *J. Phys. D. Appl. Phys*. **1993**, *26*, B242.
2. Robertson, J. M.; White, J. G. *J. Chem. Soc*. **1945**, 607.
3. Rohr, U.; Kohl, C.; Müllen, K.; van de Craats, A.; Warman, J. *J. Mater. Chem*. **2001**, *11*, 1789.
4. Rohr, U.; Schlichting, P.; Böhm, A.; Gross, M.; Meerholz, K.' Bräuchle, C.; Müllen, K. *Angew. Chem. Int. Ed.* **1998**, *37*, 1434.
5. An, Z.; Yu, J.; Domercq, B.; Jones, S. C.; Barlow, S.; Kippelen, B.; Marder, S. R. *J. Mater. Chem*. **2009**, *19*, 6688.
6. Alibert-Fouet, S.; Dardel, S.; Bock, H.; Oukachmih, M.; Archambeau, S.; Seguy, I.; Jolinat, P.; Destruel, P. *Chem. Phys. Chem*. **2003**, *4*, 983.
7. Müller, S.; Müllen, K. *Chem. Commun*. **2005**, 4045.
8. Nolde, F.; Pisula, W.; Müller, S.; Kohl, C.; Müllen, K. *Chem. Mater*. **2006**, *18*, 3715.
9. Avlasevich, Y.; Müller, S.; Erk, P.; Müllen, K. *Chem. Eur. J*. **2007**, *13*, 6555.
10. Rao, K. V.; George, S. J. *Org. Lett*. **2010**, *12*, 2656.
11. Rieger, R.; Kastler, M.; Enkelmann, V.; Müllen, K. *Chem. Eur. J*. **2008**, *14*, 6322.
12. Jia, H.-P.; Liu, S.-X.; Sanguinet, L.; Levillain, E.; Decurtins, S. *J. Org. Chem*. **2009**, *74*, 5727.
13. Li, Z.; Lucas, N. T.; Wang, Z.; Zhu, D. *J. Org. Chem*. **2007**, *72*, 3917.
14. Wei, J.; Han, B.; Guo, Q.; Shi, X.; Wang, W.; Wei, N. *Angew. Chem. Int. Ed*. **2010**, *49*, 8209.
15. Haley, M. M.; Tykwinski, R. R. *Carbon-Rich Compunds From Molecules to Materials*; Wiley-VCH; Weinheim, **2006**.
16. Dötz, F.; Brand, J. D.; Ito, S.; Gherghel, L.; Müllen, K. *J. Am. Chem. Soc*. **2000**, *122*, 7707.

17. Feng, X.; Pisula, W.; Müllen, K. *Pure Appl. Chem*. **2009**, *81*, 2203.

18. Rieger, R.; Müllen, K. *J. Phys. Org. Chem*. **2010**, *23*, 315.

19. Yang, X.; Dou, X; Rouhanipour, A.; Zhi, L.; Rader, H. J.; Müllen, K. *J. Am. Chem. Soc*. **2008**, *130*, 4216.

20. Feng, X.; Wu, J.; Ai, M.; Pisula, W.; Zhi, L.; Rabe, J. P.; Müllen, K. *Angew. Chem. Int. Ed*. **2007**, *46*, 3033.

21. Wiberg, K. B. *J. Org. Chem*. **1997**, *62*, 5720.

22. Fort, E. H.; Donovan, P. M.; Scott, L. T. *J. Am. Chem. Soc*. **2009**, *131*, 16006.

23. Langhals, H.; Kirner, S. *Eur. J. Org. Chem*. **2000**, 365.

24. Alibert-Fouet, S.; Seguy, I.; Bobo, J.-F.; Destruel, P.; Bock, H. *Chem. Eur. J*. **2007**, *13*, 1746

25. Murase, T.; Horiuchi, S.; Fujita, M. *J. Am. Chem. Soc*. **2010**, *132*, 2866.

26. Nishioka, Y.; Yamaguchi, T.; Yoshizawa, M.; Fujita, M. *J. Am. Chem. Soc*. **2007**, *129*, 7000.

27. Murase, T.; Fujita, M. *Chem. Rec*. **2010**, *10*, 342.

Chapter 3

Synthesis and self-assembly of Oilgo phenylenevinylene-Coronene bisimide-Oilgo phenylenevinylene (OPV3-Coro-OPV3) triad

Abstract

The synthesis and self-assembly study of donor-acceptor dyads and triads is known in literature for various applications. But new chromophores having better electronic and self-assembly properties are always desired for this purpose. Thus here we report on the synthesis and self-assembly of Oligo phenylenevinylene-Coronene bisimide-Oligo phenylenevinylene (**OPV3-Coro-OPV3**) triad. This molecule consists of a central coronene bisimide and two OPV molecules on either sides. This molecule self-assembles in chloroform and methanol mixture to form long fibres in solution.

3.1 Introduction

The use of organic materials as active components in electronic devices has increased over the past two decades.[1,2,3,4] So the quest for new materials possessing functional properties is an intense area of research. Also the control of morphology can play a very important role in the performance of the device. Thus approaches like the Bulk Heterojnction (BHJ) solar cells are used to provide a good interface between the Donor and Acceptor.[5] Another approach is to achieve better morphology of the active layer through the self-assembly of the active layer components. Thus the importance of this Donor-Acceptor-Donor (DAD) triad or Donor-Acceptor (DA) dyads as an attractive class of materials for applications in moleclar electronics is recognised.

Here in this chapter we look at the synthesis of Oligo (Phenylenevinylene)-Coronene bisimide-Oligo (Phenylenevinylene) (**OPV3-Coro-OPV3**) along with its optical and morphological studies.

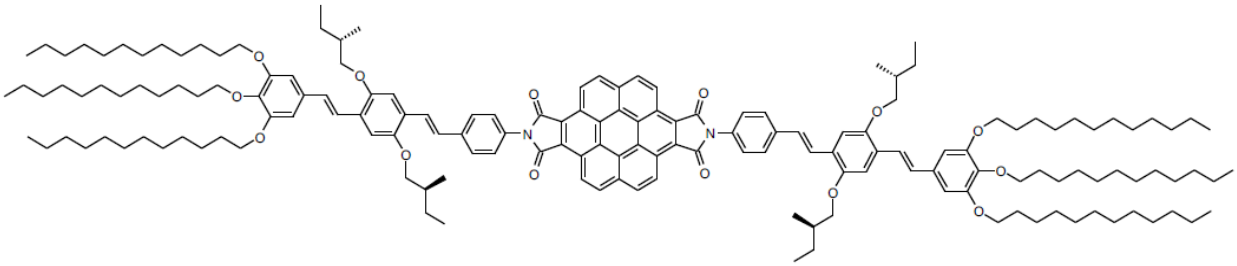

OPV3-Coro-OPV3

3.2 Synthetic schemes

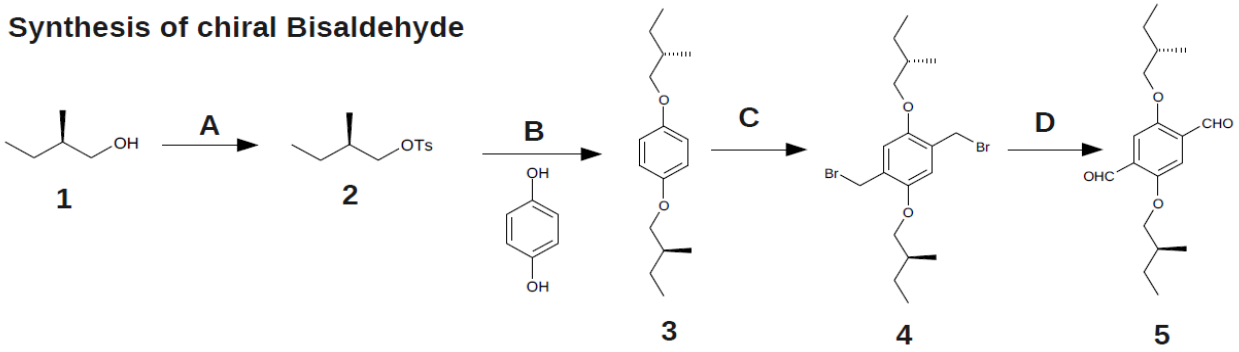

Scheme 1. (**A**) Et_3N, p-TsCl, 0 ^{0}C DCM (**B**) K_2CO_3, TBAB, 2-butanone, 90 ^{0}C, 24 h, refulx (**C**) CH_2O, HBr in Acetic acid , Acetic acid, 70 ^{0}C, 2 h (**D**) DMSO, $NaHCO_3$, 90 ^{0}C, 45 mins.

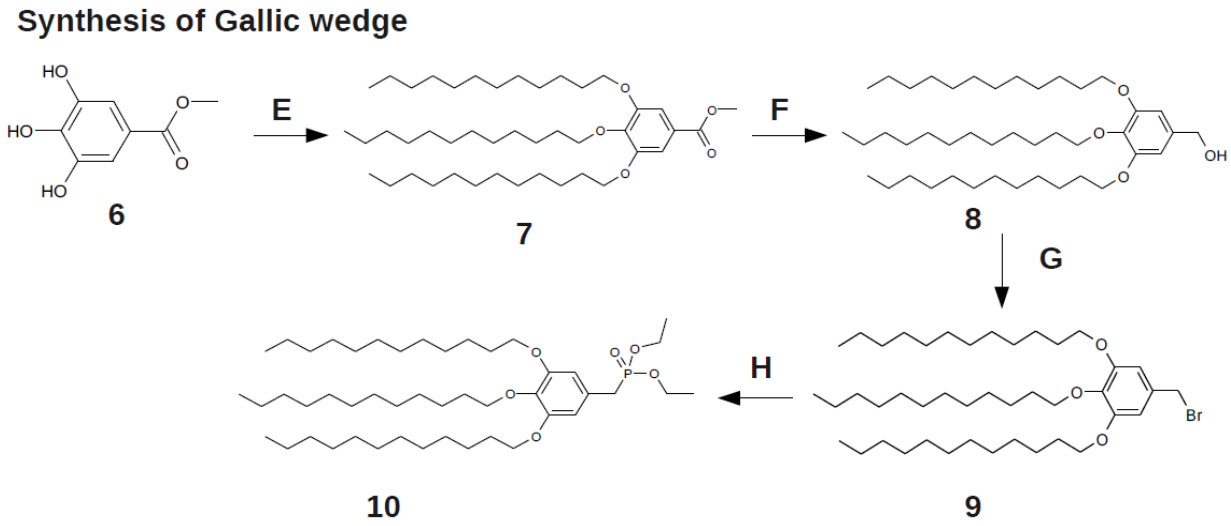

Scheme 2. (**E**) $C_{12}H_{25}Br$, K_2CO_3, DMF, 80 ^{0}C, 12 h (**F**) $LiAlH_4$, THF, 25 ^{0}C, 11 h (**G**) PBr_3, DCM, 0 ^{0}C to 25 ^{0}C, 4 h (**H**) $P(OEt)_3$, 130 ^{0}C, 12h.

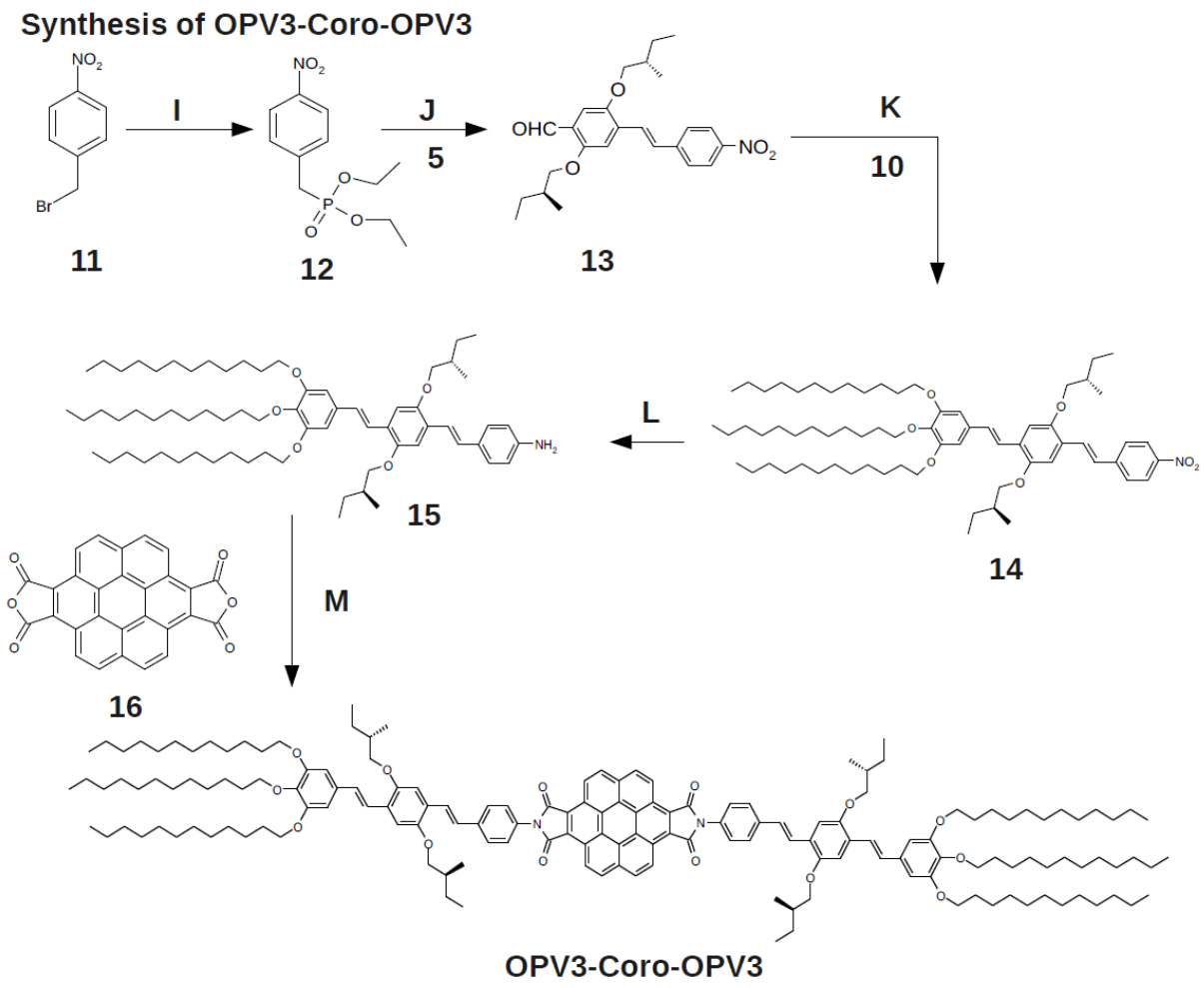

Scheme 3. (**I**) $P(OEt)_3$, 130 ^{0}C, 12h (**J**) $KO(CH_3)_3$, DMF, 12-18 ^{0}C, 2 h (**K**) $KO(CH_3)_3$, DMF/THF, 15 ^{0}C to 60 ^{0}C, 12 h (**L**) $SnCl_2$, EtOAc, EtOH, 70 ^{0}C, reflux (**M**) $ZnCl_2$, quinoline, 190 ^{0}C, 16 h.

The chiral Oligo(phenylenevinylene) (OPV3) was synthesised in a multi step process as shown in the above synthetic schemes. One of the key steps involved in the synthesis of OPV3 is the synthesis of **5**. We synthesised **5** in a very convenient way using Dimethyl Sulfoxide (DMSO) as both solvent as well as an oxidising agent.[6] This reaction is simple and non-time consuming and yields were also optimized to around 65-70 %. The synthesis of OPV2-nitro (**13**) was achieved using selective Wittg-Horner reaction in good yield. This was followed by another Wittig-Horner reaction to yield OPV3-nitro (**14**) which on reduction yielded OPV3-amine (**15**).

Coronene dianhydride (**16**) was synthesised according to a literature procedure.[7] OPV3-amine (**15**) was coupled to coronene dianhydride (**16**) using quinoline as a solvent at 190 ^{0}C to obtain **OPV3-Coro-OPV3**. All molecules were completely characterised by ^{1}H-NMR and Mass spectrometry. The MALDI-TOF of **OPV3-Coro-OPV3** is shown below (Figure 3.1), it shows the presence of $[M+2H]^{+}$ peak and other fragments corresponding to masses of 2304 and 2161. The peaks observed in the lower mass range correspond to matrix peaks.

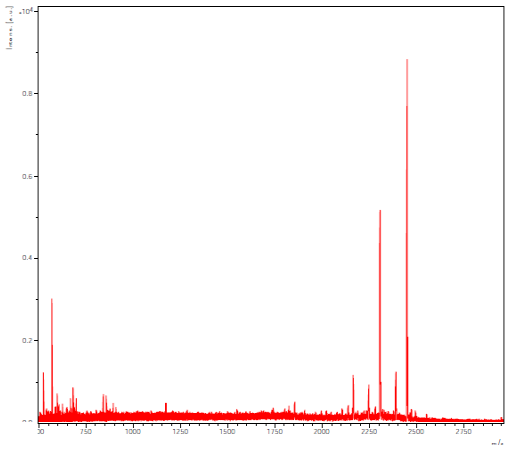

Figure 3.1 MALDI-TOF of **OPV3-Coro-OPV3**.

3.3 Self-Assembly in solution

The UV/Vis spectrum of **OPV3-Coro-OPV3** is as shown in Figure 3.2, and it has features of both coronene bisimide and OPV3. OPV3 has an absorption maxima at 406 nm due to the π-π* transition of the OPV3 moieties. It also has a high energy shoulder band around 320 nm.[8] Coronene bisimides show vibronic features from 425 nm to 500 nm and the abosrption maxima occurs around 340 nm.[9,10] **OPV3-Coro-OPV3** in its molecularly dissolved form in chloroform has three main absorption peaks, one around 340 nm corresponding to the coronene bisimide part, another around 400 nm corresponding to the OPV3 part and the characteristic vibronic features of coronene bisimide around 490 nm.

Aggregation of **OPV3-Coro-OPV3** was studied in a mixture of chloroform and methanol at a concentration of $1*10^{-5}$ M. First the compound was dissolved in a good solvent (chloroform) and then injected into the required amount of bad solvent (methanol). As the amount of methanol increases the UV/Vis absorption spectra shows a gradual lowering of the intensity for peaks at 340 nm and 400 nm, but the vibronic features around 490 nm show a gradual red shift, thus indicating the formation of aggregates. Aggregation begins at 40 % methanol and 60 % chloroform composition. On complete aggregation a 10 nm red shift is observed in the feature around 490 nm. This lowering of intenisty of peaks at 340 nm and a red shift of the vibronic band is characteristic of J-aggregates of coronene bisimides.[10] Thus we can conclude that the molecule as a whole also aggregates in the same manner.

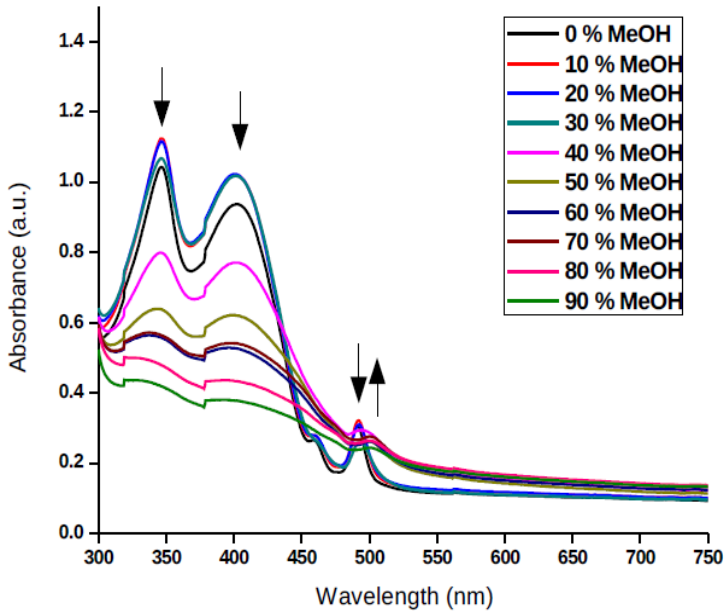

Figure 3.2 Absorption spectra of OPV3-Coro-OPV3 in methanol chloroform in 10 mm cuvette at $1*10^{-5}$ M concentration.

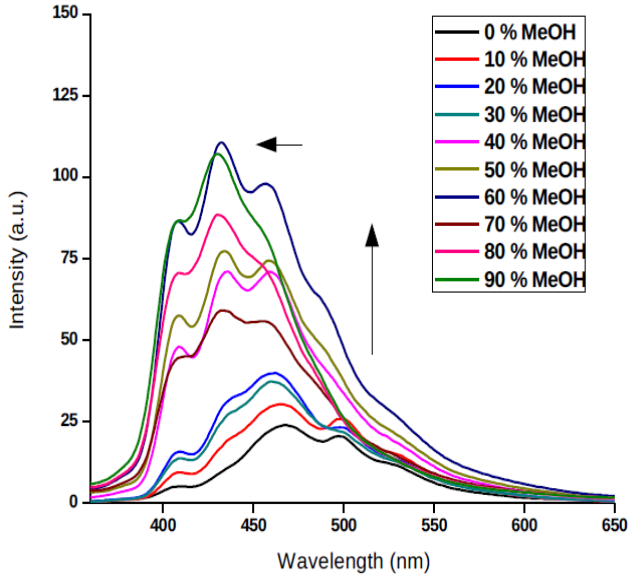

Figure 3.3 Emission spectra of OPV3-Coro-OPV3 in methanol chloroform in 10 mm cuvette at $1*10^{-5}$ M concentration (λ_{exc}=340 nm).

The emission spectra of **OPV3-Coro-OPV3** at the corresponding compositions when excited at 340 nm is as shown in Figure 3.3. From this spectra it is evident that as we go to higher amounts of methanol a blue shift accompained by an increase in fluorescence is observed. At 40 % of methanol and 60 % of chloroform the increase in fluorescence is prominent, indicating the formation of aggregation. This is contrary to what is generally expected when we observe the formation of J-aggregates through UV/Vis spectroscopy. This anomaly can be rationalised by explaining the presence of Twisted Intramolecular Charge Transfer (TICT). Initially when the molecule is in its moleculary dissolved state, the two chromophores are twisted because of steric reason and thus the charge transfer is most efficient leading to very low fluorescence. Once the molecule starts aggregating, because of the addition of methanol, aggregation induced fluorescence enhancement is observed. The observed blue shift could be because of break in the TICT as obseved in other systems.[11] This hypothesis has to be studied further using fluorescence life time to prove beyond doubt the presence of TICT in the system.

3.4 Morphological studies

The morphology of **OPV3-Coro-OPV3** was studied at $1*10^{-5}$ M in 1:1 of chloroform and methanol. The FESEM images (Figure 3.4) show the presence of fibers and clustering of these fibers to form bundles. This is in agreement with optical studies indicating the formation of aggregates. The dimension of the aggregates varies from few 100 nm to couple of microns.

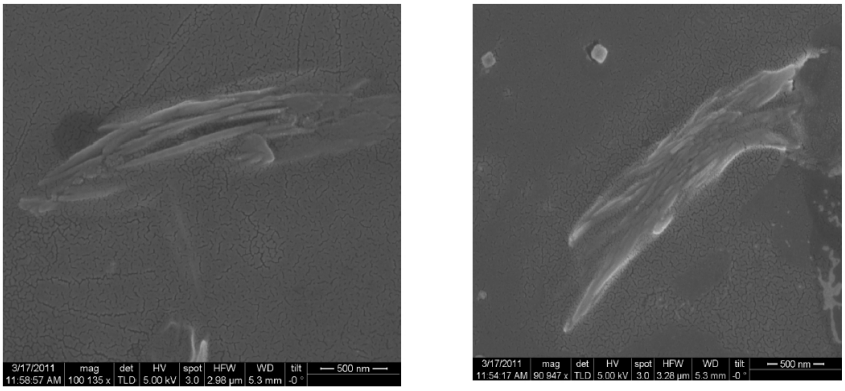

Figure 3.4 FESEM micrographs showing the formation of nanofibers and clustering of these nanofibers to form nanobundles (Conc. $1*10^{-5}$ M, 1:1 chloroform and methanol on glass substrate sputtered with gold for 20 seconds).

3.5 Conclusions and future outlook

Thus here we have shown the synthesis and self-assembly of Donor-Acceptor-Donor triad using coronene bisimide as an acceptor. This molecule self-assembles in a mixture of chloroform and methanol to form fibers and bundles. Also intramolecular charge transfer is observed in the molecularly dissolved state, which is indicated by the very low fluorescence of the molecule. Also the molecule has shown liquid crystalline properties and these aspects are currently under investigation. Future work will be aimed at fabricating transistors out of this molecule and studying it performances.

3.6 Experimetal Section

General Methods

NMR Measurements: NMR spectra were obtained with a Brucker AVANCE 400 (400 MHz) Fourier transform NMR spectrometer with chemical shifts reported in parts per million (ppm) with respect to Tetramethylsilane (TMS).

Matrix-assisted laser desorption ionization time-of-flight (MALDI-TOF): MALDI-TOF spectra were obtained on a Brucker ultraflex 2 MALDI-TOF mass spectrometer with α-cyano-4-hydroxycinnamic acid matrix.

Optical Measurements: Electronic absorption spectra were recorded on a Perkin Elmer Lambda 900 UV-Vis-NIR Spectrometer and emission spectra were recorded on Perkin Elmer Ls 55 Luminescence Spectrometer. UV-Vis and emission spectra were recorded in 10 mm path length cuvette. Fluorescence spectra were recorded with 340 nm excitation wavelength.

Field Emission Scanning Electron Microscopy (FE-SEM): FE-SEM measurements were performed on a NOVA NANO SEM 600 (FEI) by drop casting the solutions on glass substrate followed by drying in vacuum at 40 ^{0}C and were operated with an accelerating voltage of 30 kV.

Synthesis of **2**

(S)-(-)-2-methyl butanol (**1**) (10 g, 113.4 mmol), Triethylamine (34.43 g, 340. mmol) were taken in a 500 mL two necked RBF fitted with a dropping funnel and a magnetic stirrer. The mixture was stirred at 0 ^{0}C for 20 minutes. Then para-toluenesulfonyl chloride (p-TsCl) (25. 953 g, 136.13 mmol) was dissolved in 250 mL of dry DCM and added to the RBF through the dropping funnel dropwise under argon atmosphere. The reaction mixture was stirred at 0 ^{0}C for another 22 hours. After the completion of the reaction, the reaction mixture was filtered to remove the excess of p-TsCl. The solvent was removed from the filtrate under vacuum. The resulting liquid was extracted with 1 M HCl (50 mL, three times) and chloroform to remove excess of triethylamine and p-TsCl. Finally it was washed with brine and the collected organic fractions was dried over anhydrous sodium sulfate to obtain a colorless liquid. The crude product was purified by silica gel column chromatography (100-200 mesh size) in 1:1 chloroform:hexane to obtain a colorless liquid. (second spot was the product, 19 g, 70 % yield): ^{1}H-NMR (400 MHz, $CDCl_3$) δ ppm 7.78 (d, *J*=8.4 Hz, 2H, Ar-H), 7.34 (d, *J*=8 Hz, 2H, Ar-H), 3.88 (dd, *J*=6 Hz, *J*=3.2 Hz, 1H, OCH_2), 3.81 (dd, *J*=6.4 Hz, *J*=3.2 Hz, 1H, OCH_2), 2.45 (s, 3H, CH_3), 1.70 (m, 1H, CH), 1.12 (m, 1H, CH_2), 1.15 (m, 1H, CH2), 0.87 (d, *J*=6.8 Hz, 3H, CH_3), 0.82 (t, *J*=7.2 Hz, 3H, CH_3), MS, GC-MS- Retention time 16.433 mins., 242 $[M]^+$.

Synthesis of **3**

Hydroquinone (4 g, 36.36 mmol), **2** (17.6 g, 72.72 mmol), tetrabutylammonium bromide (TBAB, 1.406 g, 4.36 mmol) were taken in a 50 mL one necked RBF and sonicated thoroughly to dissolve hydroquinone. In another 250 mL two necked RBF potassium carbonate (30.15g, 218.18 mmol) and 2-butanone was taken. The reaction mixture (hydroquinone+**2**+TBAB) was added to this two necked RBF through a syringe under argon atmosphere. The reaction

mixture was refluxed at 90 ^{0}C for 24 hours. Once the reaction mixture cooled down to room temperature it was filtered and and washed with chloroform to dissolve the product sticking to unreacted potassium carbonate. The filtrate was evaporated under vacuum to obtain a dark liquid. The crude product was purified by a silica gel (100-200 mesh size) chromatography using 30 % chloroform and 70 % hexane as the eluent to obtain a colorless liquid (first fraction, 5.9 g, 65 % yield): ^{1}H-NMR (400 MHz, $CDCl_3$) δ ppm 6.81 (s, 4H, Ar), 3.76 (dd, *J*=6 Hz, *J*=2.8 Hz, 2H, OCH_2), 3.67 (dd, *J*=6.4 Hz, *J*=2.8 Hz, 2H, OCH_2), 1.82 (m, 2H, CH), 1.41 (m, 2H, CH_2), 1.24 (m, 2H, CH_2), 0.99 (d, *J*=6.8 Hz, 6H, CH_3), 0.93 (t, *J*=7.6 Hz, 6H, CH_3).

Synthesis of **4**

3 (5.9 g, 23.6 mmol) was taken in a 250 mL single necked RBF and 80 mL of acetic acid is added to it. Then paraformaldehyde (1.559 g, 51.92 mmol) and HBr in acetic acid (9. 377 mL) was added at once and the mixture was refluxed for 2 hours at 70 ^{0}C. Once it cooled down to room temperature the reaction mixture (already containing white needdle shaped crystals) is poured into a beaker containing ice cold water. The precipitate was filtered under suction. The precipitate was then extracted with water and chloroform till the water layer becomes neutral to pH. The collected organic fractions were dried over anhydrous sodium sulfate and evaporated under vacuum to obtain a pale yellow solid (10.28 g, 80 % yield): ^{1}H-NMR (400 MHz, $CDCl_3$) δ ppm 6.84 (s, 2H, Ar), 4.52 (s, 4H, CH_2Br), 3.84 (dd, *J*=6 Hz, *J*=2.8 Hz, 2H, OCH_2), 3.77 (dd, *J*=6 Hz, *J*=2.8 Hz, 2H, OCH_2), 1.89 (m, 2H, CH), 1.60 (m, 2H, CH_2), 1.33 (m, 2H, CH_2), 1.06 (d, *J*=6.8 Hz, 6H, CH_3), 0.96 (t, *J*=7.4 Hz, 6H, CH_3).

Synthesis of **5**

4 (6.81 g, 15.9 mmol) was taken in 500 mL two necked RBF and to this dimethyl sulfoxide (DMSO, 200 mL) and $NaHCO_3$ (26.25 g, 312.38 mmol) was added and the mixture was heated at 90 ^{0}C for 45 mins. **4** is insoluble in DMSO, thus it floats initially and goes into the solution as the reaction proceeds. During the course of the reaction bubbles start emerging, indicating the evolution of HBr. The reaction is continued till the bubbles evolution stops. Then it is allowed to cool to room temperature and extracted with diethyl ether to obtain an yellow colored liquid. A silica gel (100-200 mesh size) chromatography was performed using 20 % chloroform and 80 % of hexane as the eluent to obtain a yellow solid (3.28 g, 67 % yield): ^{1}H-NMR (400 MHz, $CDCl_3$) δ ppm 10.53 (s, 2H, CHO), 7.43 (s, 2H, Ar), 3.95 (dd, *J*=6 Hz, *J*=2.8 Hz, 2H, OCH_2), 3.88 (dd, *J*=6.4 Hz, *J*=2.8 Hz, 2H, OCH_2), 1.93 (m, 2H, CH), 1.57 (m, 2H, CH_2), 1.33 (m, 2H, CH_2), 1.04 (d, *J*=6.8 Hz, 6H, CH_3), 0.92 (t, *J*=7.6 Hz, 6H, CH_3).

Synthesis of **7**

3,4,5-trihydroxy benzoate (**6**) (10 g, 54.347 mmol), 1-bromododecane (54. 1826 g, 217.39 mmol) and potassium carbonate (52. 51 g, 380. 43 mmol) were taken in a 1000 mL three necked RBF fitted with a condenser and a magnetic stirrer. 220 mL of dry DMF was added to the RBF under argon atmosphere and the reaction mixture was heated at 80 ^{0}C for 12 hours. The reaction mixture was allowed to cool down to room temperature and then it was poured into 600 mL of ice cold water. This water solution was extracted with hexane and washed with brine. The collected organic fractions were dried over anhydrous sodium sulfate and evaporated under vacuum to obtain a dark colored liquid. This crude product was purified by precipitation. About 700 mL of methanol was taken in a 1000 mL beaker and cooled to 0 ^{0}C. The crude product dissolved in chloroform was added slowly to the solution drop wise while stirring, instantly the formation of a

white precipitate was observed with the upper layer gaining the dark color. The solution was filtered under suction and washed with excess of methanol. The precipitate was dried under vacuum at 70 ^{0}C to get pure white solid (37.35 g, quantitative yield): ^{1}H-NMR (400 MHz, $CDCl_3$) δ ppm 7.24 (s, 2H, Ar-H), 3.67 (tt, *J*=2.8 Hz, *J*=2.8 Hz, 6H, gallic OCH_2), 3.88 (s, 3H, $0CH_3$), 1.84-1.75 (m, 6H, CH_2), 1.26 (m, 54H, gallic CH_2), 0.87 (t, *J*=6.4 Hz, 9H, CH_3).

Synthesis of **8**

Lithium aluminiumhydride ($LiAlH_4$, 0.689 g, 18.16 mmol) was taken in a three necked 100 mL RBF connected to a condenser, dropping funnel and a magnetic stirrer. The RBF is purged with argon gas. Then 15 mL of dry tetrahydrofuran (THF) was added under argon atmosphere. While adding THF the RBF is maintained at 0-5 ^{0}C by using ice-bath. $LiAlH_4$ is paritially soluble in THF as it is coated with a polymer. To dissolve it completely the mixture was stirred for 2 hours at room temperature (25 ^{0}C). **7** (10 g, 14.53 mmol) is dissolved in 25 mL of dry THF in a 100 mL single necked RBF and transfered to the dropping funnel. This solution was added dropwise under argon atmosphere while maintaining the temperature of the RBF between 0-5 ^{0}C. Then the mixture was stirred at room temperature (25 ^{0}C) for 11 hours.

Again the RBF was maintained between 0-5 ^{0}C and a 1:1 mixture of methanol and water was added dropwise to quench the reaction. 2 mL of this 1:1 mixture was enough to quench the reaction completely (effervescence stops). The resulting solution is diluted with water and a saturated solution of sodium potassium tartarate (Rochelle's salt) is added to it and stirred at room temperature for about half an hour. This breaks the emulsion formed by aluminium leading to an aluminium tartarate complex which is soluble in water and the product precipitates out. The precipitate is filtered off under suction and dried under vacuum at 50 ^{0}C for 24 hours to obtain white

solid (9.5 g, quantitative yield): ^{1}H-NMR (400 MHz, $CDCl_3$) δ ppm 6.55 (s, 2H, Ar-H), 4.59 (d, *J*=6 Hz, 2H, CH_2OH), 3.98-3.91 (m, 6H, OCH_2), 1.82-1.69 (m, 6H, CH_2), 1.26 (m, 54H, gallic CH_2), 0.87 (t, *J*=6.8 Hz, 9H, CH_3).

Synthesis of **9**

8 (10.30 g, 15.60 mmol) was taken in 250 mL two necked RBF fitted with a dropping funnel and a magentic stirrer. 60 mL of dry dichloromethane (DCM) is added to the RBF under argon atmosphere and stirred at 0 ^{0}C for 45 mins. Phosphorous tribromide (8.448 g, 31.21 mmol) was dissolved in 8 mL of dry DCM and added to the RBF dropwise through dropping funnel under argon atmosphere at 0 ^{0}C. The reaction mixture turned to brown color after half an hour. Then the ice bath was removed and the reaction mixture was stirred at 25 ^{0}C for 4 hours. Then the mixture was poured into 400 mL of double distilled water taken in a 1000 mL beaker. A brown liquid settled at the bottom. This solution was extracted with chloroform and water, the combined organic fractions were dried over anhydrous sodium sulfate and evaporated under vacuum to obtain a brownish white (off-white) solid (8.9 g, 85 % yield): ^{1}H-NMR (400 MHz, $CDCl_3$), δ ppm 6.57 (s, 2H, Ar-H), 4.43 (s, 2H, CH_2Br), 3.97-3.91 (m, 6H, OCH_2), 1.82-1.72 (m, 6H, CH_2), 1.26 (m, 54H, gallic CH_2), 0.87 (t, *J*=6.4 Hz, 9H, CH_3).

Synthesis of **10**

9 (8.9 g, 12.30 mmol) and triethyl phosphite (2.25 g, 13.54 mmol) were taken in a 50 mL single necked RBF fitted with a condenser and a magnetic stirrer. The mixture is heated at 130 ^{0}C for 12 hours under argon atmoshpere. The reaction mixture is allowed to come down to room temperature and an oily liquid was obtained (8.88 g, quantitative): ^{1}H-NMR (400 MHz, $CDCl_3$) δ ppm 6.49 (s, 2H, Ar-H), 3.99-3.89 (m, 6H, OCH_2), 3.04 (d, *J*=21.2 Hz, 2H, PCH_2), 1.81-1.68

(m, 6H, CH_2), 1.26 (m, 54H, gallic CH_2), 0.87 (t, *J*=6.8 Hz, 9H, CH_3).

Synthesis of **12**

para-nitrobenzyl bromide (**11**) (5 g, 23.14 mmol) and triethylphosphite (4.23 g, 25.45 mmol) were taken in a 50 mL one necked RBF connected to a condender and a magnetic stirrer. The reaction mixture was heated at 130 ^{0}C for 12 hours under argon atmosphere. The reaction mixture is allowed to cool down and a dark colored oil was obtained (6.31 g, quantitative): ^{1}H-NMR (400 MHz, $CDCl_3$) δ ppm 8.17 (d, *J*=8.8 Hz, 2H, Ar-H), 7.46 (dd, *J*=8.8 Hz, *J*=2.4 Hz, 2H, Ar-H), 4.05 (m, 4H, OCH_2), 3.23 (d, *J*=22 Hz, 2H, PCH_2), 1.26 (t, *J*=7.2 Hz, 6H, CH_3).

Synthesis of **13**

5 (500 mg, 1.633 mmol) and **12** (375 mg, 1.373 mmol) were taken in a 100 mL three necked RBF fitted with a dropping funnel and a magnetic stirrer. 16.5 mL of dry DMF was added under argon atmosphere. The reaction was maintained at around 15 ^{0}C. Potassium tertiary butoxide (225 mg, 2 mmol) was dispersed in 12.5 mL of dry DMF and transfered to the dropping funnel. This solution was added drop wise while stirring with sufficient interval of time to allow for the disappearance of the color of anion (dark red) formed. It is very important to maintain a very slow rate of addition to prevent the formation of both side nitro product. Then the solution was stirred at this temperature for another 2 hours. The reaction mixture was then poured into 100 mL of 3N HCl and extracted with diisopropyl ether and water and finally washed with brine. The collected organic fractions were dried over anhydrous sodium sulfate and evaporated under vacuum to obtain orange to red colored liquid. The crude product was purified by silica gel (100-200 mesh size) chromatography using 60 % chloroform and 40 % hexane as the eluent to obtain a dark orange colored solid (525 mg, 90 % yield): ^{1}H-NMR (400 MHz, $CDCl_3$) δ ppm 10.48 (s, 1H, CHO), 8.24

(d, *J*=8.8 Hz, 2H, Ar-H), 7.65 (d, *J*=8.8 Hz, 2H, Ar-H), 7.61 (d, *J*=16.8 Hz, 1H, vinylic proton) 7.35 (s, 1H, Ar-H), 7.31 (d, *J*=16.4 Hz, 1H, vinylic proton), 7.17 (s, 1H, Ar-H), 4.00-3.90 (m, 4H, OCH_2), 2.00-1.90 (m, 2H, CH), 1.64-1.5 (m, 2H, CH_2), 1.39-1.31 (m, 2H, CH_2), 1.08 (d, *J*=6.8 Hz, 6H, CH_3), 0.98 (t, *J*=7.6 Hz, 6H, CH_3).

Synthesis of **14**

10 (3.02 g, 38.77 mmol) and potassium tertiary butoxide (1.1602 g, 10.34 mmol) was taken in a three necked RBF fitted with a condenser, dropping funnel and a magnetic stirrer. 30 mL of dry DMF was added to the RBF under argon atmosphere and stirred for 30 mins. **13** (1.1 g, 2.585 mmol) was dissolved in 20 mL of dry DMF and transfered to the dropping funnel. This solution was added dropwise to the RBF. The reaction mixture became really dark after the addition of **13**. The reaction mixture was heated to 60 ^{0}C for 12 hours. After the reaction cooled down to room temperature THF was evaporated and the rest was poured into 200 mL of 3 N HCl. This solution was extracted with diisopropyl ether and washed with brine. The combined organic fractions were dried over anhydrous sodium sulfate and evaporated under vacuum to obtain orange colored paste (1.8 g, 67 %): ^{1}H-NMR (400 MHz, $CDCl_3$) δ ppm 8.22 (d, *J*=8.8 Hz, 2H, Ar-H), 7.64 (d, *J*=16.4 Hz, 1H, vinylic proton), 7.61 (d, *J*=4 Hz, 2H, Ar-H), 7.37 (d, *J*=16.4 Hz, 1H, vinylic proton), 7.19 (d, *J*=16.4 Hz, 1H, vunylic proton), 7.11 (s, 1H, Ar-H), 7.10 (s, 1H, Ar-H), 7.05 (d, *J*=16.4 Hz, 1H, vinylic proton), 6.74 (s, 2H, Ar-H), 4.03-3.84 (m, 10H, OCH_2), 1.96-1.92 (m, 2H, CH), 1.86-1.79 (m, 8H, CH_2), 1.26 (m, 54H, gallic CH_2), 1.11 (dd, *J*=2 Hz, *J*=6.4 Hz, 6H, CH_3), 1.01 (tt, *J*=2.4 Hz, *J*=7.6 Hz, 6H, CH_3), 0.88 (t, *J*=6.8 Hz, 9H, CH_3); MALDI-TOF MS m/z 1051 $[M]^+$, 1074 $[M+Na]^+$ Calcd for $C_{68}H_{109}NO_7$ 1051.

Synthesis of **15**

14 (600 mg, 0.57088 mmol), tin chloride (1.288 g, 5.7088 mmol), ethyl acetate (10 mL) and ethanol (10 mL) were taken in a 50 mL two necked RBF fitted with a condenser and a magnetic stirrer. The mixture was heated at 70 ^{0}C for 4 hours. The orange color of the solution slowly turned to red and then dark red over a period of half an hour of heating. Once the reaction mixture comes down to room temperature it was poured into 100 mL of 0.1 M sodium hydroxide and extracted with chloroform and water. The combined organic fractions were dried over anhydrous sodium sulfate and evaporated under vacuum to obtain a dark red colored paste. The crude product was purified by silica gel (100-200 mesh size) chromatography using 80 % chloroform and 20 % hexane as the eluent to obtain an orange colored paste (470 mg, 81 % yield): ^{1}H-NMR (400 MHz, $CDCl_3$) δ ppm 7.37 (d, *J*=16 Hz, 1H, vinylic proton), 7.34 (d, *J*=8.4 Hz, 2H, Ar-H), 7.28 (d, *J*=16 Hz, 1H, vinylic proton), 7.08 (s, 1H, Ar-H), 7.07 (s, 1H, Ar-H), 7.05 (d, *J*=16.8 Hz, 1H, vinylic protons), 6.99 (d, *J*=16.4 Hz, 1H, vinylic proton), 6.73 (s, 2H, Ar-H), 6.68 (d, *J*=8 Hz, 2H, Ar-H), 4.03-3.80 (m, 10H, OCH_2), 1.97-1.93 (m, 2H, CH), 1.85-1.73 (m, 8H, CH_2), 1.26 (m, 54H, gallic CH_2), 1.10 (d, *J*=6.8 Hz, 6H, CH_3), 0.99 (t, *J*=7.2 Hz, 6H, CH_3), 0.88 (t, *J*=6.8 Hz, 9H, CH_3); MALDI-TOF MS m/z 1022 $[M+H]^+$ Calcd for $C_{68}H_{111}NO_5$ 1021.

Synthesis of **OPV3-Coro-OPV3**

15 (435 mg, 0.426 mmol), coronene dianhydride (**16**) (75 mg, 0.170 mmol), zinc chloride (24 mg, 0.17045 mmol) and 5 mL of dry quinoline were taken in a 25 mL single necked RBF and heated at 190 ^{0}C under argon atmosphere for 16 hours. After the reaction was over, it was allowed to come down to room temperature and methanol was added to obtain a dark brown precipitate. The crude product was subjected to a silica gel (100-200 mesh size) chromatography in 80 % chloroform and 20 % hexane as eluent to remove the base spot. Another silica gel (100-200

mesh size) chromatography was performed on the first fraction of the last column with same eluent of 80 % chloroform and 20 % hexane. The fractions obtained from this column are subjected to repeated size exclusion chromatography (Biobeads, SX-1, THF) for many cycles to obtain the pure product as an orange pasty solid (70 mg, 17 % yield): ^{1}H-NMR (400 MHz, $CDCl_3$) δ ppm 9.80 (d, *J*=8.4 Hz, 4H, Coronene Ar-H), 8.72 (d, *J*=8.8 Hz, 4H, Coronene Ar-H), 7.90 (d, *J*=8 Hz, 4H, OPV3 Ar-H), 7.81 (d, *J*=8.4 Hz, 4H, OPV3 Ar-H), 7.58 (d, *J*=16.4 Hz, 2H, vinylic proton), 7.28 (d, *J*=16 Hz, 2H, vinylic proton), 7.11 (s, 2H, Ar-H), 6.91 (s, 2H, Ar-H), 6.8-6.4 (m, 4H, vinylic proton), 6.55 (s, 4H, gallic Ar-H), 4.00-3.83 (m, 20H, OCH_2), 1.87-1.80 (m, 4H, CH), 1.783-1.70 (m, 16H, CH_2), 1.27 (m, 108H, gallic CH_2), 1.19 (d, *J*=6.8 Hz, 12H, CH_3), 1.12 (d, *J*=6.8 Hz, 12H, CH_3), 1.09 (t, *J*=7.2 Hz, 12H, CH_3), 1.03 (t, *J*=7.2 Hz, 12H, CH_3), 0.89 (t, *J*=6 Hz, 18H, CH_3); MALDI-TOF MS m/z 2448 $[M+2H]^+$ Calcd for $C_{164}H_{226}N_2O_{14}$ 2446.

3.7 References

1. Lo, S.-C; Burn, P. L. *Chem. Rev*. **2007**, *107*, 1097.
2. Gunes, S.; Neugebauer, H.; Sariciftci, N. S. *Chem. Rev*. **2007**, *107*, 1324.
3. Brunetti, F. G.; Kumar, R.; Wudl, F. *J. Mater. Chem*. **2010**, *20*, 2934.
4. Wu, W.; Liu, Y.; Zhu, D. *Chem. Soc. Rev*. **2010**, *39*, 1489.
5. Würthner, F.; Meerholz, K. *Chem. Eur. J*. **2010**, *16*, 9366.
6. Shao, P.; Li, Z.; Luo, J.; Wang, H.; Qin, J. *Synth. Commun.* **2005**, *35*, 49.
7. Alibert-Fouet, S.; Seguy, I.; Bobo, J.-F.; Destruel, P.; Bock, H. *Chem. Eur. J*. **2007**, *13*, 1746.
8. Peeters, E. PhD thesis, TU/e, Eindhoven, **2000**.
9. An, Z.; Yu, J.; Domercq, B.; Jones, S. C.; Barlow, S.; Kippelen, B.; Marder, S. R. *J. Mater. Chem*. **2009**, *19*, 6688.
10. Rao, V. K.; George, S. J. *Org. Lett*. **2010**, *12*, 2656.
11. Yang, X.; Lu, R.; Zhou, H.; Xue, P.; Wang, F.; Chen, P.; Zhao, Y. *J. Colloid Interface Sci*. **2009**, *339*, 527.

PART B

Theoretical study of supramolecular polymerisation in Benzene-1,3,5-tricarboxamides

Chapter 1

Introduction

Abstract

The self-assembly of small molecules into larger macromolecular structures is important in many fields within chemistry and biology. These synthetic macromolecules are used to mimic natural counterparts and they have also gained a lot of technological importance recently. Thus in this chapter, an account of supramolecular polymers and the mechanisms of supramolecular polymerisation is given. Also an introduction is given to the theoretical methods employed in the present thesis.

1.1 Supramolecular polymers

Supramolecular polymers date back to the times of Jean Marie Lehn when his group synthesised the first supramolecular polymer using triple hydrogen bonding between difunctional diaminopyridines and difunctional uracils in early 1990s.[1,2] The monomers in the supramolecular polymers possess highly directional non-covalent interactions. They can exhibit polymer properties both in solution as well as in bulk. The heart of supramolecular polymers lies in the reversiblity of non-covalent interactions leading to dynamic polymers. The term supramolecular polymers was coined so as to distinguish them from the conventional living polymers. On the one hand, the reversibility of the interaction has an advantage that they can be used as stimuli responsive materials, but on an another the reversibility also brings down the polymer properties.[3,4,5,6] A schematic of conventional and supramolecular polymers is shown in Figure 1.1. The main differences between conventional or covalent polymers and the supramolecular polymers are (1) The conventional polymers exhibit good material properties, whereas supramolecular polymers do not show such good material properties. (2) The conventional polymers generally undergo polymerisation under kinetic control, thus the barrier for the backward reaction is too high, which is consistant with the observed low reversibility. But in case of supramolecular polymers the polymerisation takes place under thermodynamic control leading to a greater degree of reversibility.

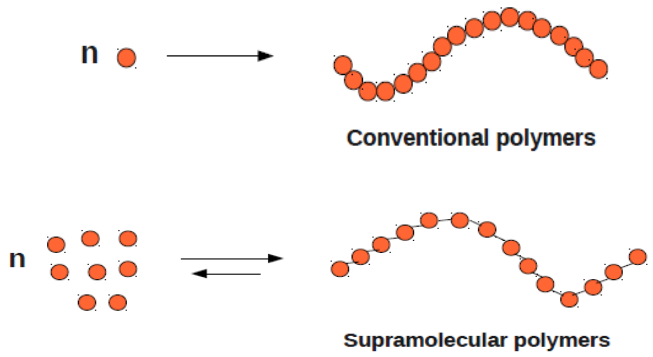

Figure 1.1 A schematic of conventional and supramolecular polymers.

Supramolecular polymers are defined as " polymeric arrays of monomeric units that are brought together by reversible and highly directional secondary interactions, resulting in polymeric properties in dilute and concentrated solutions, as well as in the bulk. The monomeric units of the supramolecular polymers themselves do not possess a repetition of chemical fragments. The directionality and strength of the supramolecular bonding are important features of the systems that can be regarded as polymers and that behave according to well-established theories of polymer physics ".[3]

Supramolecular polymers can be classified based on the structural properties of the monomeric units and also on the nature of the interactions possible between the monomers. The first class involves diotopic or multifunctional groups as monomers. In a diotopic monomer two functional groups can be separated by a spacer or can be directly linked. With the help of directional complimentary couple (A-B) or self-complimentary couple (A-A) it is possible to form all structures of conventional polymers like homo and coopolymers,[7] cross linked polymers and even hyperbranched structures.[8] The degree of polymerisation (DP) of supramolecular polymers containing bifunctional monomers is determined by the strength of the end group interaction. The DP is dependent on the concentration of the solution and the association constant of the monomer units as can be seen from Figure 1.2. In order to obtain high molecular weight supramolecular polymers, the association constant between the monomers should be high. Monofunctional monomers can be added to control the extent of polymerisation and thus the molecular weight. Since the presence of monofunctional monomers stops the polymerisation by acting as "chain stoppers" it is always desirable to start with a pure difunctional monomer, because during the synthesis of difunctional monomer, monofunctional monomer can act as impurity.

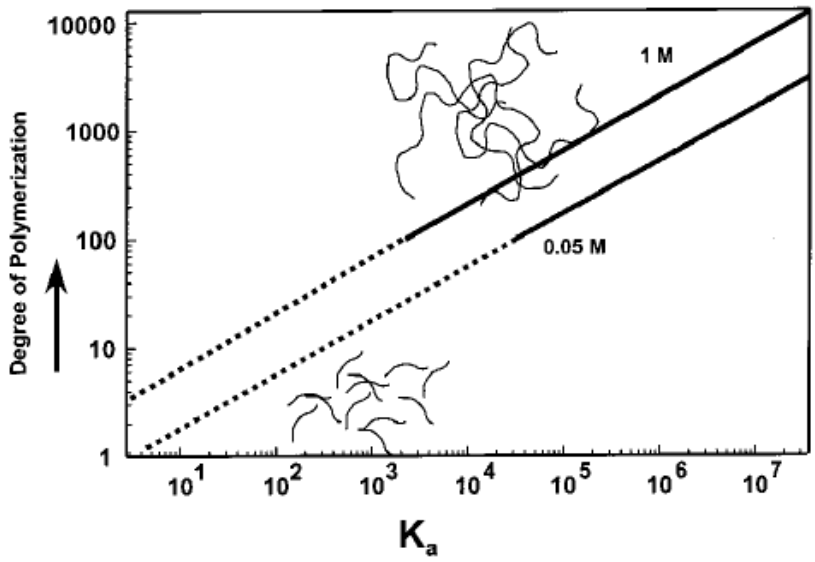

Figure 1.2 Theoretical plot of Degree of Polymerisation (DP) vs the association constant k_a.[3]

Many class of molecules have been used for supramolecular polymers based on the nature of the intermolecular interactions like hydrogen bonding, arene-arene interaction and metal-ligand interactions. Among all the supramolecular polymers, the ones based on hydrogen bonding have attracted a lot of attention from both experimental[9] as well as theoretical point[10,11] of view because of their materials properties. A variety of hydrogen bonded arrays can be constructed including multiple hydrogen bonds operating in synergy to give different morphologies as well as material properties reminiscent of conventional polymers.[12,13] Some of the examples of hydrogen bonded supramolecular polymers are calix[4]arene dicyanuric acid and calix[4]arene dimelamine based,[14] benzene-1,3,5-tricarboxamide based,[15,16,17] calixarene based,[18,19,20] ureidopyrimidinone based,[21,22] etc. The possible material applications of these polymers are as rheology modifiers, adhesives, adsorbents, coatings, surfactants, and stabilizers.

Other interactions like arene-arene interaction based supramolecular polymers are also known and are based on discotic molecules. Here the discotic molecule contains the peripheral

self-assembling side chains and the core provides the direction for stacking. These can also exhibit liquid crystalline nature in the solid or melt. Some of the molecules capable of such polymerisation are triphenylenes,[23] extended core phthalocyanines[24] and porphyrins,[25] helicenes,[26,27,28] m-phenylene ethynylene oligomers[29,30] etc. Some of the large aggregates of the above molecules are also called as supramolecular polymers. Another class of supramolecular polymers is the supramolecular coordination polymers. Here the monomers have metal binding sites and this can extend in one dimension to give a large supramolecular coordination polymer. Typical monomers capable of undergoing such polymerisation are phenanthroline based,[31] porphyrin based,[32] polycyclic ether based,[33] etc. A pure hydrophobic interaction based supramolecular polymer was obtained using β-cyclodextrins and diphenylhexatriene (DPH).[34] Here the β-cyclodextrins are arranged in a linear array and the DPH molecules are accomodated in the inner hydrophobic cavity of β-cyclodextrins leading to the one-dimensional arrangement.

This new branch of polymer chemistry has grown at a rapid pace and is no longer just a scientific curiosity, new applications of these supramolecular polymers is foreseen to be technologically important. Also one or more intermolecular forces like arene-arene and hydrogen bonding can act in synergy to enhance the properties of the polymers.

1.2 Mechanisms in supramolecular polymerisation

As the field of supramolecular polymers expanded many polymers showed low polydispersity index (PDI) and high molecular weight, only with a subtle change in molecular structure the PDI and thus the molecular weight distribution varied. This stems from the strength of interaction between the monomer units and also the nature of intermolecular interactions present.

Thus it becomes important to decipher the mechanisms of polymerisation to understand them in terms of the basic intermolecular interactions. So the quest for understanding these mechanisms began with the early work of van der Schoot and coworkers involving mainly analytical theories applied to helical transition in one-dimensional polymers,[35] and to the problem of chirality amplification in supramolecular systems using one-dimensional Ising model.[36,37]

The supramolecular polymerisation mechanisms can be divided based on (1) The nature of the intermolecular interaction which governs the polymerisation. (2) Type of the monomer i,e. monofunctional, bifunctional or multifunctional. (3) Thermodynamics of the polymerisation i,e variation in change in Gibbs free energy as a function of oligomer size.[38,39,40] The last classification seems the most appropriate and tractable. Based on this criteria of variation of the change in Gibbs free energy as a function of oligomer size the mechanisms can be classified into three types namely Isodesmic polymerisation, ring-chain polymerisation and Cooperative polymerisation as shown in Figure 1.3. Each of these mechanisms are explained below.

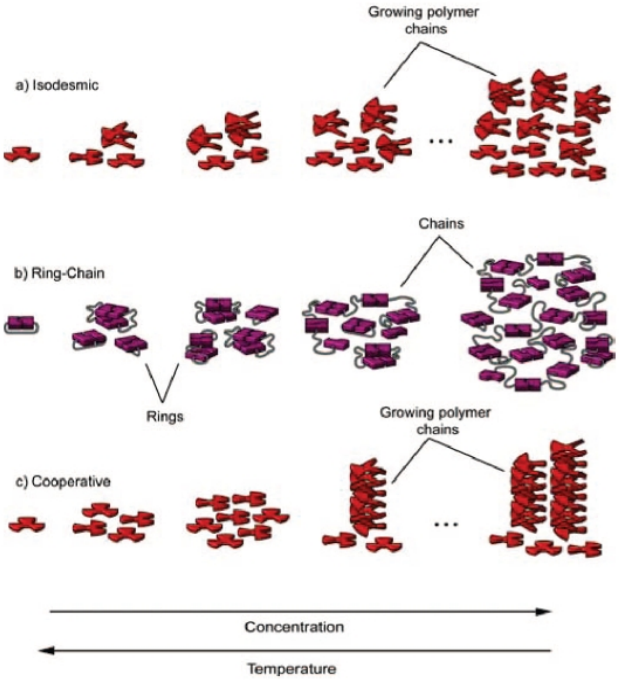

Figure 1.3 Graphical representation of the three growth mechanism of supramolecular polymer.[38]

1.2.1 Isodesmic supramolecular polymerisation

Isodesmic polymerisation involves the formation of a reversible non-covalent interaction between monomers, the strength of which remains the same irrespective of the size of the oligomer. This means that the reactivity of the end groups does not change during supramolecular polymerisation and the presence of other molecules also has no effect on non-nearest neighbours. Isodesmic supramolecular polymerisation is also characterised by the absence of cyclic intermediates. Iso means equal and desmic means bond, in other words the strength of interaction or the association constant is equal for every subsequent addition of the monomer as shown in the equations below.[41]

$$M_1 + M_1 \overset{K}{\rightleftharpoons} M_2 \qquad [M_2]=K[M_1]^2$$

$$M_2 + M_1 \overset{K}{\rightleftharpoons} M_3 \qquad [M_3]=K^2[M_1]^3$$

$$M_{i-1} + M_i \overset{K}{\rightleftharpoons} M_i \qquad [M_i]=K^{i-1}[M_1]^i \quad i=1,2,3,.....\infty$$

Since the association constant is same for all the steps, this type of poymerisation does not show any critical temperature or critical concentration where polymerisation shows an abrupt change. Thus the DP also increases with increase in concentration or decrease in temperature. This is best monitored by following a curve of fraction of polymer or aggregate as a function of temperature or concentration (Figure 1.4(a)). This curve is sigmoidal for isodesmic polymerisation. This kind of polymerisation is analogous to step-growth polymerisation in conventional polymers. As with step growth polymers, here also even at high concentration or low temperature enough monomers will be left unused resulting in a high PDI value. As a result of this,

it is difficult to obtain high molecular weight polymers, with polymers formed by this kind of mechanism. Also the molecular weight distribution is broad with a single peak.

From a thermodynamics point of view, the change in Gibbs free energy of formation of the polymer always decreases monotonically (Figure 1.4 (b)). This is understandable because an equal association constant relates to a monotonic change in free energy.

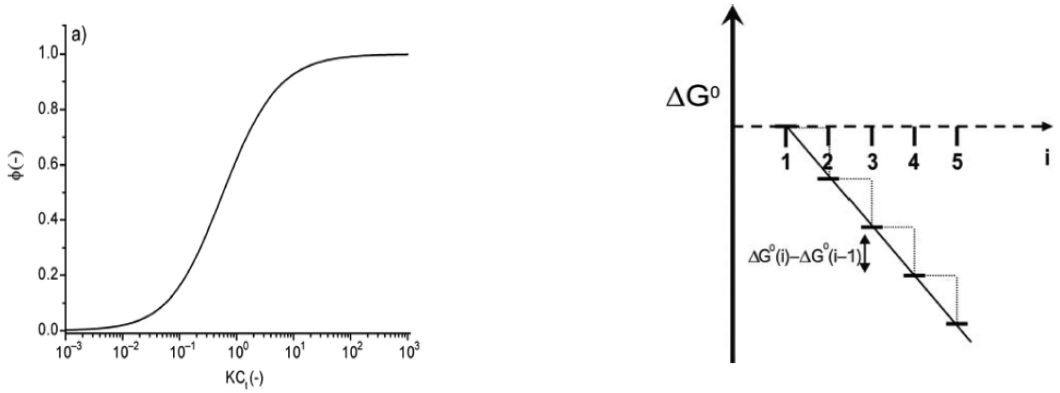

(a) (b)

Figure 1.4 (a) Fraction of aggregation vs dimensionless association constant (b) Change in Gibbs free energy vs oligomer size for an isodesmic model. [38]

There are many different examples of isodesmic supramolecular polymers, to name a few of them, C_3 symmetrical acylated 3,3'-diamino-2,2'-bipyridine substituted benzene-1,3,5-tricarboxamides,[42] some of the perylenebisimide derivatives[43] and phenylacetylene macrocycles.[44]

1.2.2 Ring-Chain polymerisation

This second class of supramolecular polymers consist of a ditopic monomer with or without a spacer. During the reversible polymerisation of a ditopic monomer linear aggregates are in equilibrium with cyclic conterparts as shown in the Figure 1.5 There will always be a

competition between the ring formation and the chain formation during the course of the polymerisation. Unlike isodesmic supramolecular polymerisation, this class exhibits a critical temperature or critical concentration. At this critical temperature there is a transition in equilibrium between cyclic species and high molecular weight chains.

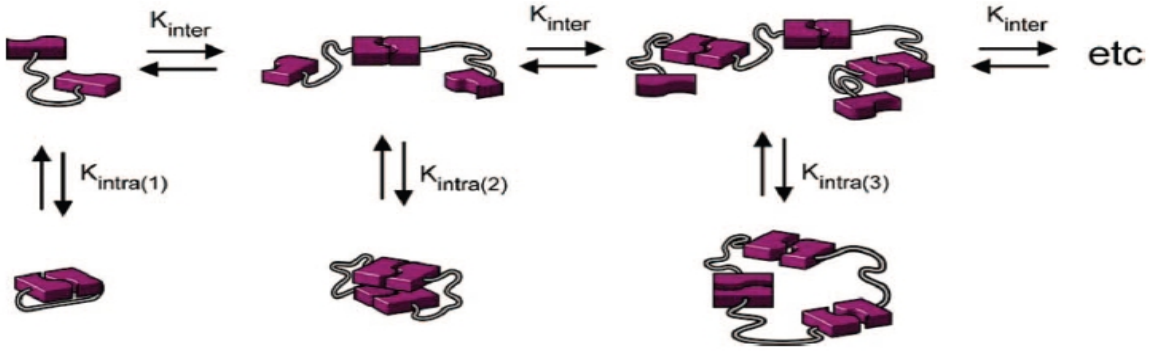

Figure 1.5 A schematic of ring-chain polymerisation.[38]

The nature of the spacer linking the two functionality is critical in forming the cyclic oligomers in solution and solid state. Examples of this type of polymerisation include bifunctional ureidopyrimidinone based on m-xylylene linkers.[45]

1.2.3 Cooperative supramolecular polymerisation

In this kind of polymerisation, a bifunctional monomer undergoes polymerisation to form one-dimensional stacks. The mechanism is characterised by two equilibrium constants, one for nucleation and another for elongation. This mechanism also involves a critical temperature or critical concentration above which elongation takes place.[46] This class of polymerisation involves the formation of a nucleus containing a critical number of molecules, the formation of nucleus is thermodynamically unfavourable. But once the nucleus is formed, then it is a down hill process in terms of Gibbs free energy leading to the formation of large stacks. Thus the association constant

(K_n) for the nucleus formation is less than the association constant (K_e) of the elongation as can be seen from below equations. In other words, cooperativity can be quantified by the ratio of K_n/K_e, if this value is lower than 1 then it follows a cooperative polymerisation, here n indicates the size of the nucleus.[38]

$$M_1 + M_1 \overset{K_2}{\rightleftharpoons} M_2 \qquad [M_2]=K_2[M_1]^2$$

$$M_2 + M_1 \overset{K}{\rightleftharpoons} M_3 \qquad [M_3]=KK_2[M_1]^3$$

$$M_{i-1} + M_i \overset{K}{\rightleftharpoons} M_i \qquad [M_i]=K_2K^{i-2}[M_1]^i=\sigma K^{-1}(K[M_1])^i$$

$$i=1,2,3,.....\infty$$

Cooperativity can be classified into two types mainly electronic cooperativity and structural cooperativity. In case of electronic cooperativity, electronic properties like the bond polarisabilities and hydrogen bond strength change during the course of polymerisation. Examples of this class are known even in classical conventional polymers. In case of structural cooperativity, the polymerisation is initially unfavourable and becomes favourable once the polymer attains a certain length beyond which the polymer grows into an ordered structure. Examples of such polymerisation include self-assembly of the tobacco mosaic virus and polymerisation of G-actin into fibrous F-actin in natural systems. This kind of cooperativity has gained importance in supramolecular polymers only recently.[47]

Based on the variation of change in Gibbs free energy as a function of oligomer size, cooperative polymerisation is further classified into nucleation-elongation polymerisation and cooperative down hill polymerisation (Figure 1.6 (a) and Figure 1.6 (b)).

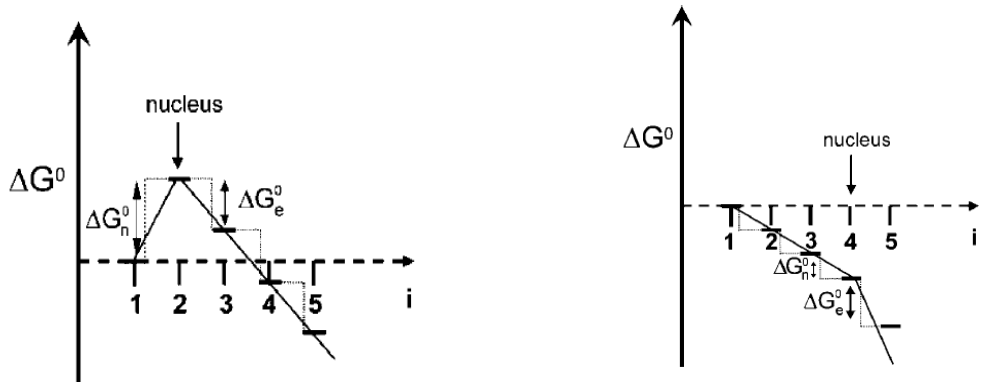

(a) (b)

Figure 1.6 (a) Cooperative nucleation-elongation mechanism (b) cooperative downhill polymerisation.[38]

Because of the presence of critical concentration or critical temperature, the graph of fraction of aggregate versus the concentration or temperature looks non-sigmoidal (Figure 1.7 (a)). Thus this mechanism can be conveniently monitored using temperature dependence of aggregation at a given particular wavelength. Also distribution of DP for cooperative polymerisation is bimodal because of the presence of small oligomers or nucleus during polymerisation (Figure 1.7 (b)).

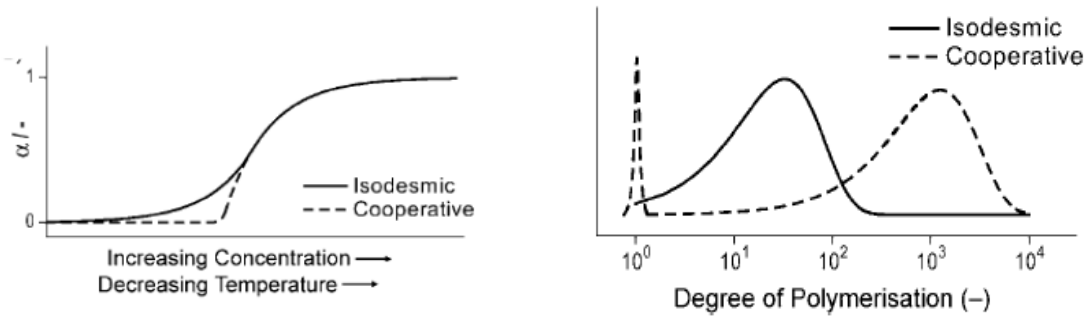

Figure 1.7 (a) Fraction of aggregation vs concentration or temperature[39]

(b) Distribution of Degree of Polymerisation[39]

1.3 Theoretical background

1.3.1 Density Functional Theory (DFT)

Quantum mechanics provides the framework for the calculation of the different properties of atoms and molecules by solving the full Schrödinger equation of the system. But this task of solving the Schrödinger equation of the system can be computationally very expensive and in many cases even it is impossible. To circumvent this problem, there were early attempts of approximation like the Hartree-Fock theory. In this theory, it is assumed that each electron sees all other electrons as an average field. This simplification, although a crude one leads to the calculation of more realistic practical systems but without the inclusion of electron-electron correlation. More rigorous post Hartree-Fock approaches like the Moller-Plesset perturbation theory, which treats the correlation as a perturbation to the Fock operator and the Configuration Interaction methods are introduced, but they are computationally very expensive. In the wake of the these developments, a computationally less demanding, more accurate and conceptually sound theory was developed, called the Density Functional Theory (DFT).

The cornerstone of DFT lies in the use of ground state density of the system to express the full ground state wavefunction and ground state energy of the system. Since the electron density of a system is a function in itself of the coordinates of the system and also the total integration of this electron density over the space occupied by the system gives the total number of electrons in the system, it has all the ingredients to express the wavefunction in terms of electron density. Two very important theorems explain this connection between the electron density of the system and the wavefunction and also about its practicability.[48,49]

1.3.1.1 The Hohenberg-Kohn theorem

The Hohenberg-Kohn (HK) theorem gives the conceptual foundation for relating the density and wavefunction of the system to calculate the other observables.

The first theorem states that " The external potential $V_{ext}(\vec{r})$ is a unique function of $\rho(\vec{r})$ since in turn $V_{ext}(\vec{r})$ fixes $\hat{H}$ we see that the full many particle ground state is a unique functional of $\rho(\vec{r})$ "[50]

i,e $\rho_0 \Rightarrow (N, Z_A, R_A) \Rightarrow \hat{H} \Rightarrow \psi_0 \Rightarrow E_0$ (and all other properties) (1.1)

Since the complete ground state energy is a functional of the ground state electron density, other components of the hamiltonian should also be the functional of ground state electron density (1.1).

$$E_0[\rho_0] = T[\rho_0] + E_{ee}[\rho_0] + E_{Ne}[\rho_0] \tag{1.2}$$

where (1.2) the first term is the kinetic energy term, second term is the energy due to electron-electron repulsion and third is energy due to the electron-nucleus attraction.

It is convenient at this point to separate the terms which are specific to a system, like the potential energy term arising from the electron-nucleus attraction from the system independent terms. Thus the above equation modifies as

$$E_0[\rho_0] = \int \rho_0(\vec{r}) V_{Ne} \, d\vec{r} + T[\rho_0] + E_{ee}[\rho_0] \tag{1.3}$$

The first term in (1.3) is system dependent and the other two terms are universally valid. This collection of last two terms is called the Hohenberg-Kohn functional $F_{HK}[\rho_0]$ (1.5)

$$E_0[\rho_0] = \int \rho_0(\vec{r}) V_{Ne} \, d\vec{r} + F_{HK}[\rho_0] \tag{1.4}$$

$$F_{HK}[\rho_0] = T[\rho_0] + E_{ee}[\rho_0] \tag{1.5}$$

$$E_{ee} = J[\rho] + E_{ncl}[\rho] \tag{1.6}$$

In equation (1.6), the first term is the classical Coulomb part and the second is the non-classical contribution to electron-electron interaction.

The Hohenberg-Kohn functional (1.5) is the most important equation of DFT. This functional contains the kinetic energy as a functional of density and electron-electron correlation. The exact functional form of these two terms is not know, it is here that the approximations starts to creep in in DFT.

Till now what we saw was, if we know the ground state electron density then we can calculate any ground state observable or properties of interest. But how sure are we that what ever density we have is that of the ground state? To answer this question we look at the second Hohenberg-Kohn theorem.

The second theorem states that "The Hohenberg-Kohn functional $F_{HK}[\rho_0]$ that delivers the ground state energy of the system, delivers the lowest energy if and only if the input density is the true ground state density, ρ_0 ". This is nothing but the variational principle of quantum mechanics.

Thus the main framework of the DFT is given by these two theorems which tell us about a unique mapping between the ground state density ρ_0 and the ground state energy E_0 . But the Hohenberg-Kohn theorems do not provide any guidance about the construction of the functionals which provide the ground state energy.

1.3.1.2 Kohn-Sham approach

Kohn-Sham developed an elegant approach to handling the difficult kinetic energy term of the Hohenberg-Kohn functional. This approach does not aim at calculating the exact kinetic energy but makes a trade-off between the accuracy and the computational demand. They suggested

the use of exact kinetic energy expression (1.7) of the non-interacting system with the same density as the real system.

$$T_S = -(\frac{1}{2})\sum_i^N \langle \phi_i | \nabla^2 | \phi_i \rangle \tag{1.7}$$

The non-interacting kinetic energy is not same as the true kinetic energy of the interacting system, even if the densities are same. Thus to account for this, an extra interacting part is introduced in (1.5) calling it the exchange-correlation energy term.[51]

$$F[\rho(\vec{r})] = T_S[\rho(\vec{r})] + J[\rho(\vec{r})] + E_{XC}[\rho(\vec{r})] \tag{1.8}$$

The exchange-correlation part of the term contains electron-electron interaction and the extra term correcting for interaction in kinetic energy.

$$E_{XC}[\rho(\vec{r})] \equiv (T[\rho] - T_S[\rho]) + (E_{ee}[\rho] - J[\rho]) = T_C[\rho] + E_{ncl}[\rho] \tag{1.9}$$

In (1.9) the residual part of true kinetic energy is T_C .

Thus the Schrödinger equation for non-interacting single particle Kohn-Sham Hamiltonian is given by

$$H_{KS}\Phi_i(\vec{r}) = \epsilon_i \Phi_i(\vec{r}) \tag{1.10}$$

here $$H_{KS} = -(\frac{\hbar^2}{2\mathrm{m}})\nabla^2 + V_{ext}(\vec{r}) + V_{Hartree}[\rho(\vec{r})] + V_{XC}[\rho(\vec{r})] \tag{1.11}$$

and thus $$\rho(\vec{r}) = \sum_i^N |\Phi_i(\vec{r})|^2 \tag{1.12}$$

The E_{XC} contains not only, the non-classical effects of the self-interaction correction, exchange and correlation, which are contributions to the potential energy of the system, but also a portion pertaining to kinetic energy is also included in it. Over the past few decades many exchange-correlation functionals have been developed for a variety of problems. Local Density

Approximation (LDA) and Generalised Gradient Approximation (GGA) are the popularly used class of approximations to the exchange correlation functionals.

1.3.2 Geometry optimization and basis sets

Geometry optimization is essentially a search for the minimum energy configuration of the system. In DFT geometry optimization, first the Kohn-Sham equations are solved to obtain the energy at each step. This total energy is used to calculate the forces on each atom by using Hellmann-Feynman theorem, i.e. a derivative of total energy with respect to atomic coordinates. This procedure is repeated till the forces and the maximum displacements (in some sense represents the maximum stress) reach below a threshold value.

To solve the Kohn-Sham equations, electronic wavefunctions are generally expanded in a basis set. These basis sets are a bunch of mathematical functions used to represent the system. There are many types of basis sets like plane wave, localised functions and a mixture of both plane wave and localised functions. The choice of the basis set depends on the system of interest. The more the number of basis set functions chosen to represent the system better the accuracy, ideally basis set should be infinite, but seldom this is practically possible.

Localised basis sets are generally used for molecular systems or non-periodic systems and the plane wave basis sets are an obvious choice for periodic systems because of the periodicity built in in the functions. Plane wave basis sets do not suffer from Basis Set Superposition Error (BSSE) but the localised ones have to be corrected for this. BSSE is an error which occurs in the binding energy calculation of clusters of atoms or molecules. This is because

the number of wavefunctions used for calculating the total energy of the cluster is more than that used for the components. This reflects in the energy of the cluster being lower (without BSSE correction the binding energy will always be the lower bound on binding energy). So as to account for this use of different number of basis set functions, one has to perform the BSSE correction to obtain the correct binding energies.[49]

The use of DFT becomes increasingly expensive if one wants to model a large system, thus other computationally less demanding techinques like molecular dynamics are suitable for problems involving large number of atoms. This is also called molecular mechanics approach.

1.3.3 Molecular Mechanics

Molecular mechanics involves the study of molecules using classical equations of motion. It involves the use of force field to describe the different possible interactions in the system. Force field is an expression involving all the possible interactions in the system. In molecular mechanics, only the evolution of the system over a period of time is monitored without the breaking or formation of new covalent bonds. The main application of molecular mechanics is to the study of systems which involve the configurational changes like in proteins or in self-assembly were weak intermolecular interactions are operating. It is also used to calculate a number of bulk properties of systems which may not be easily accessible to experiments.

The force field used to describe a given system generally involves terms which explain the bonding, angles, dihedrals, out-of plane bending, non-bonded interaction and electrostatic interactions within a molecule.

$$U=\sum_{bonds}(\frac{1}{2})k_{AB}(R_{AB}-R_{e,B})^2+\sum_{angles}(\frac{1}{2})k_{ABC}(\theta_{ABC}-\theta_{e,ABC})^2+\sum_{dihedrals}(\frac{U_0}{2})(1-\cos(n(\chi-\chi_0)))$$

$$+\sum_{outofplane}(\frac{k}{(2\sin^2\psi_e)})(\cos\psi-\cos\psi_e)^2 \quad +\sum_{nonbonded}(\frac{C}{R})_{AB}^{12}-(\frac{C}{R})_{AB}^{6} \quad +(\frac{1}{(4\pi\epsilon_0)})\sum_{charges}(\frac{Q_A*Q_B}{R_{AB}}) \quad (1.13)$$

The general form of a force field is as shown above (1.13) with all its contributions. Depending on the particular requirement, additional terms can be added to it. Also there are mainly two ways of performing molecular mechanics, one in which all the atoms are considered explicitly called the all-atom type molecular mechanics and the other in which a group of atoms is considered as a superatom thus reducing the number of degrees of freedom of the system. The latter approach is applied when exceedingly large systems are to be simulated without compromising on the accuracy of calculation. Thus molecular mechanics is a very versatile tool to study large macroscopic systems with a microscopic level of understanding.[52]

1.4 Aim of the thesis

The present work detailed in this thesis is concerned about the elucidation of the different mechanisms in supramolecular polymerisation of benzene-1,3,5-tricarboxamide family using multiple computational techniques. A subtle variation of the interaction leads to a change in the mechanism of polymerisation in this case. This aspect of intermolecular interactions governing the mechanism of polymerisation is highlighted in this work.

1.5 References

1. Fouquey, C; Lehn, J.-M.; Levelut, A.-M. *Adv. Mater.* **1990**, *2*, 254.
2. Lehn, J.-M. *Makromol. Chem. Macromol. Symp.* **1993**, *69*, 1.
3. Brunsveld, L.; Folmer, B. J. B.; Meijer, E. W.; Sijbesma. R. P. *Chem. Rev.* **2001**, *101*, 4071.
4. Moore, J. S. *Curr. Opin. in Colloid Interface Sci.* **1999**, *4*, 108.
5. de Greef, T. F. A.; Meijer, E. W. *Nature* **2008**, *453*, 171.
6. Reith, S.; Baddeley, C.; Badijic, J. D. *Soft Matter*, **2007**, *3*, 137.
7. Klok. H.-A.; Lecommandoux S. *Adv. Mater.* **2001**, *13*, 1217.
8. Cordier, P.; Tournilhac F.; Soulie-Ziakovic, C.; Leibler L. *Nature*, **2008**, *451*, 977.
9. Sijbesma, R. P.; Meijer, E. W. *Curr. Opin. Colloid Interface Sci.* **1999**, *4*, 24.
10. Jorgensen, W. L; Pranata, J. *J. Am. Chem. Soc.* **1990**, *112*, 2008.
11. Pranata, J.; Weirschke, S. G.; Jorgensen, W. L. *J. Am. Chem. Soc.* **1991**, *113*, 2810.
12. Sherrington, D. C; Taskinen, K. A. *Chem. Soc. Rev*. **2001**, *30*, 83.
13. Folmer, B. J. B.; Sijbesma, R. P.; Versteengen, R. M.; van der Rijit, J. A. J.; Meijer, E. W. *Adv. Mater.* **2000**, *12*, 874.
14. Kolk, A.-H.; Jolliffe, K. A.; Schauer, C. L.; Prins, L. J.; Spatz, J. P.; Moller, M.; Timmerman, P.; Reinhoudt, D. N. *J. Am. Chem. Soc.* **1999**, *121*, 7154.
15. Fitie, C. F. C; Roelofs, W. S. C.; Kemerink, M; Sijbesma R. P. *J. Am. Chem. Soc.* **2010**, *130*, 6892.
16. Mes, T.; Smulders, M. M. J.; Palmans, A. R. A.; Meijer, E. W. *Macromolecules* **2010**, *43*, 1981.
17. Stals, P. J. M.; Everts, J. C.; de Bruijn, R.; Filot, I. A. W.; Smulders, M. M. J.; Martin Rapun, R.; Pidko E. A.; de Greef, T. F. A.; Palmans, A. R. A; Meijer, E. W. *Chem. Eur. J*. **2010**, *16*, 810.

18. Castellano, R. K.; Rebek, J., Jr. *J. Am. Chem. Soc.* **1998**, *120*, 3657.

19. Castellano, R. K; Nuckolls, C.; Eichhorn, S. H.; Wood, M. R.; Lovinger, A. J.; Rebek, J., Jr. *Angew. Chem. Int. Ed.* **1999**, *38*, 2603.

20. Castellano, R. K.; Clark, R.; Craig, S. L.; Nuckolls, C.; Rebek, J., Jr. Proc. Natl. Acad. Sci. U. S. A. **2000**, *97*, 12418.

21. Sijbesma, R. P.; Beijer, F. H.; Folmer, B. J. B.; Hirschberg, J. H. K. Ky; Lange, R. F. M.; Lowe, J. K. L.; Meijer, E. W. *Science*, **1997**, *278*, 1601.

22. Folmer, B. J. B; Cavini, E.; Sijbesma, R. P.; Meijer, E. W. *Chem. Commun.* **1998**, 1847.

23. Gallivan, J. P.; Schuster, G. B. *J. Org. Chem.* **1994**, *60*, 2423.

24. van der Pol, J. F.; Neelman, E.; van Miltenburg, J. C.; Zwikker, J. W.; Nolte, R. J. M.; Drenth, W.; *Macromolecules*, **1990**, *23*, 155.

25. Fuhrhop, J.-H.; Demoulin, C.; Boettcher, C.; Koning, J.; Siggel, U. *J. Am. Chem. Soc.* **1992**, *114*, 4159.

26. Nuckolls, C.; Katz, T. J.; Castellanos, L. J. *Am. Chem. Soc.* **1996**, *118*, 3767.

27. Lovinger, A. J.; Nuckolls, C.; Katz, T. J. *J. Am. Chem. Soc.* **1998**, *120*, 264.

28. Nuckolls, C.; Katz, T. J.; katz, G.; Collings, P. J.; Castellanos, L. *J. Am. Chem. Soc.* **1999**, *121*, 79.

29. Nelson, J. C.; Saven, J. G.; Moore, J. S. Wolynes, P. G. *Science*, **1997**, *277*, 1793.

30. Brunsvel, L.; Meijer, E. W.; Prince, R. B.; Moore, J. S. *J. Am. Chem. Soc*. **2001**, *123*, 7978.

31. Velten, U.; Rehahn, M. *Chem. Commun.* **1996**, 2639.

32. Michelsen, U.; Hunter, C. A. *Angew. Chem. Int. Ed.* **2000**, *39*, 764.

33. Yamaguchi, N.; Gibson, H. W. *Angew. Chem. Int. Ed.* **1999**, *38*, 143.

34. Li, G.; McGown, L. B. *Science*, **1994**, *264*, 249.

35. van der Schoot, P.; Michels, M. A. *Langmuir*, **2000**, *16*, 10076.

36. van Gestel, J.; van der Schoot, P.; Michels, M. A. J. *Macromolecules* **2003**, *36*, 6668.

37. van Gestel, J. *Macromolecules* **2004**, *37*, 3894.

38. de Greef, T. F. A.; Smulders, M. M. J.; Wolffs, M.; Schenning, A. P. H. J.; Sijbesma, R. P.; Meijer, E. W. *Chem. Rev.* **2009**, *109*, 5687.

39. Smulders, M. M. J.; Nieuwenhuizen, M. M. L.; de Greef, T. F. A.; van der Schoot, P.; Schenning, A. P. H. J.; Meijer, E. W. *Chem. Eur. J*. **2010**, *16*, 362.

40. Chen, Z.; Lohr, A.; Saha-Moller, C. R.; Würthner, F. *Chem. Soc. Rev*. **2009**, *38*, 564.

41. Martin, R. B. *Chem. Rev.* **1996**, *96*, 3043.

42. Metzroth, T.; Hoffmann, A.; Martin-Rapun, R.; Sumlders, M. M. J.; Pieterse, K.; Palmans, A. R. A.; Vekemans, A. J. M. Jef; Meijer, E. W.; Spiess, H. W.; Gauss, J. *Chem. Sci*. **2011**, *2*, 69.

43. Würthner, F.; Thalacker, C.; Diele, S.; Tschierske, C. *Chem. Eur. J*. **2001**, *7*, 2245.

44. Zhao, D.; Moore, J. S. *Chem. Commun*. **2003**, 807.

45. Folmer, B. J. B.; Sijbesma, R. P.; Kooijman, H.; Spek, A. L.; Meijer, E. W. *J. Am. Chem. Soc.* **1999**, *121*, 9001.

46. Zhao, D.; Moore, J. S. *Org. Biomol. Chem*. **2003**, *1*, 3471.

47. de Greef, T. F. A. PhD thesis, TU/e Eindhoven **2010**.

48. Koch, W.; Holthausen, M. C. *A chemists Guide to Density Functional Theory*; Wiley; Weinheim, **2001**.

49. Cramer, C. J.; *Essentials of Computational Chemistry*; Wiley; Weinheim, **2004**.

50. Hohenberg, P.; Kohn, W. *Phys. Rev*. **1964**, *136*, B864-B871.

51. Kohn, W.; Sham, L. J. *Phys. Rev.* **1965**, *140*, A1133.

52. Hinchliffe, A.; *Molecular Modelling for Beginners*; Wiley; United Kingdom, **2009**.

Chapter 2

Co-operativity in the Stacking of Benzene-1,3,5-tricarboxamides

Abstract

Quantum chemical and force field based calculations have been carried out to study oligomerisation and cooperativity in oligomers of benzene-1,3,5-tricarboxamides (BTA). The stabilisation energy of these stacks decreases monotonically and converged value around -27.07 kcal/mol is obtained for molecule **1** (BTA). Comparison between density functional theory and MP2 level calculations for a dimer indicates the significant contribution of dispersive interactions in this system. Large oligomers have thus been studied with DFT augmented by empirical van der Waals corrections. Convergence of the stabilization energy requires a minimum of thirty molecules in a stack, as observed from force field based calculations. Similar calculations carried out on a derivative of BTA which exhibits intramolecular hydrogen bonds shows that intermolecular hydrogen bonding is crucial for cooperativity. The link between these results and experimentally established polymerization mechanisms is explored.

2.1 Introduction

Benzene-1,3,5-tricarboxamides (BTA) are a versatile class of supramolecular polymers.[1-4] They self-assemble into 1-dimensional fibers in solution,[5,6] in the solid state,[7,8] in liquid crystalline phases,[9,10] and also some of them form low molecular weight organogels depending on the nature of the substituents on the amide group.[11,12] They have also been used to study concepts of chiral amplification such as the "sergeant and soldiers" principle[13,14] and "majority rules"[15,16] in helical self-assembled systems. Due to the ease of synthesis, a wide variety of BTA homologues are accessible. In addition, the presence of amide groups and the stacking of these molecules in solution make them ideal model systems for the study of mechanisms of self-assembly that are operative in many biological systems possessing a similar functionality. Inspite of numerous reports dealing with their self-assembly and structure-property relationships, there are only a few reports[17,18] which deal with the mechanism of self-assembly.

Here, we have carried out quantum chemical as well as empirical force field based calculations to study the stacking behaviour and cooperativity in BTA. The molecule studied **1** does not have any substituents on the amide nitrogen so as to reduce the computational requirement. Thus, this is the simplest member of the BTA family exhibiting all features such as hydrogen bonding (HB) and π-π interaction; one obvious omission is the van der Waals (vdW) interaction between the substituents on the amide nitrogen, which is expected to contribute significantly less to the stabilization of the stack than the other interactions. Factors involved in the oligomerization of **1** are contrasted against those for a similar molecule, **2**; however, **2** possesses intramolecular hydrogen bonds. Thus, the oligomerization of **2** can proceed only through π-π interactions.

Earlier pioneering attempts to study the stacking of substituted benzene molecules focussed their attention to small oligomers.[19,20,21,22] de Greef and coworkers[23] have recently examined cooperativity in supramolecular aggregates in the BTA family, induced through intermolecular hydrogen bonding, using density functional theory. They demonstrate that non-additive effects play a role apart from electrostatic interactions in the cooperative growth of the stack. Their calculations, employing the PBE functional, were carried out for oligomers containing one to seven molecules in the stack. In the current work, we build on these observations. We provide results from B3LYP and PBE functional based calculations for oligomers up to a decamer. Additional calculations have also been carried out by augmenting the PBE functional with empirical vdW corrections. These have been shown to be crucial in the accurate description of weakly bound complexes such as the ones described here. Calculations for the dimer have also been performed using the MP2 method which serve as a benchmark for the results based on DFT. Further, results from a preliminary force field are provided for larger oligomers.

2.2 Computational Details

Electronic structure calculations were performed within density functional theory (DFT) using the Gaussian-03 package.[24] The geometry optimizations were carried out using B3LYP hybrid functional and 6-31+g(d,p) basis set. These are shown in the literature to capture weak HBs fairly well.[25,26] Basis set superposition error (BSSE) in energy was calculated using the counterpoise method. Larger oligomers were studied using the PBE functional[27] with a plane wave basis set as implemented in the CPMD code.[28] The energy cutoff for the expansion of wave function was 85 Ry. The oligomers were studied under isolated conditions using a tetragonal box of linear

dimensions of 40 Å, 14 Å, 14 Å along the x, y and z directions respectively. The Hockney method [29] was used to solve the Poisson equation. Initial configurations of the oligomers were in a stacked geometry with the stack axis oriented along the Cartesian x-axis. In the CPMD calculations, the effect of the nuclei and the core electrons on the valence shell was treated using norm conserving Troullier-Martins pseudopotentials. At the optimized geometry, the maximum force component on any atom was below $4.5*10^{-4}$ a.u. Dipole moments of stacks were calculated using the Berry's phase formalism[30] as implemented in the CPMD code. Empirical force field calculations were carried out using the LAMMPS package[31] using a modified, generalised CHARMM force field.[32] The CHARMM force field has been developed to study proteins and lipids. We found that its use led to short intermolecular distances for the dimer. However, employing the site charges from B3LYP calculations of a monomer as atom charges in the force field, led to considerable improvement in the intermolecular distance of the dimer. Hence, these charges were used for higher oligomers as well. The initial coordinates for the force field based geometry optimizations was obtained from earlier quantum chemical calculations. Improper dihedrals are not included in the force field because of the lack of parameters for our system from the generalised CHARMM force field.[32] Molecular Dynamics (MD) simulations were performed at 5 K using a time step of 0.5 fs for 50 ps. Velocity Auto Correlation Function (VACF) is obtained from the MD trajectory. A Fourier transform of VACF gives the Vibrational Density of States (VDOS). Using this VDOS, different contributions to the entropy are calculated. All molecules were visualised through Visual Molecular Dynamics (VMD) version 1.8.7.[33]

2.3 Results and discussion

2.3.1 Molecular assembly

In literature, weak HB has been treated with different ab initio methods and also using various basis sets.[34,35,36] The B3LYP hybrid functional represented in a basis containing diffuse and polarisable basis functions is expected to describe weak hydrogen bonding fairly well.[37] Also recently, results using a plane wave basis set are shown to be in reasonably good agreement with those obtained from localised gaussian basis sets,[38] although the former makes use of periodic boundary conditions. Thus we have made use of the plane wave basis set functions to perform electronic structure calculations of higher oligomers.

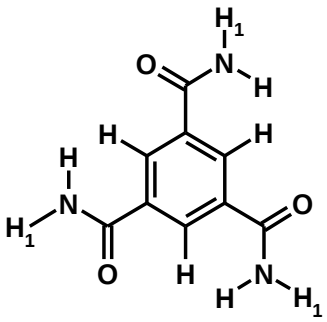

Benzene-1,3,5-tricarboxamide (**1**)

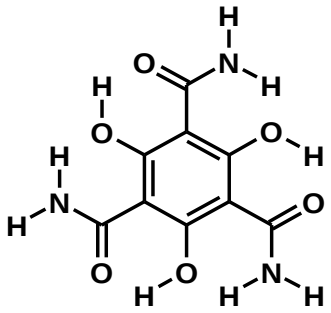

2,4,6-Trihydroxy-benzene-1,3,5-tricarboxamide (**2)**

Figure 2.1 Molecules under study

The molecules under study are shown in Figure 2.1 Both molecules are nearly planar. We started with different initial conformations of **1** for the optimization, but all of them lead to a minimum energy planar structure. This planarity in geometry is reflected in the small value of its dipole moment (0.149 D). The stability offered by oligomerization has been quantified using the

definition of "stabilization energy", defined as $SE=(E_n - n*E_1)/(n-1)$ where n is the number of molecules in the oligomer. Dimerization of **1** proceeds through the formation of three intermolecular hydrogen bonds and results in a large value of SE as seen in Figure 2.2. SE decreases with increasing n and should eventually converge to a bulk value. On fitting the stabilization energies obtained from the PBE/85 Ry calculations to a polynomial, a "bulk" (i.e., converged) SE value of around -17.018 kcal/mol is obtained, which is comparable to the value of 17.68 kcal/mol obtained for an infinite chain of trimethyl substituted BTA using same PBE functional by de Greef and coworkers.[23] The SE curve for the B3LYP functional exhibits a similar rate of convergence as the PBE curve; however its values are estimated to be lower by about 4 kcal/mol than the PBE result.

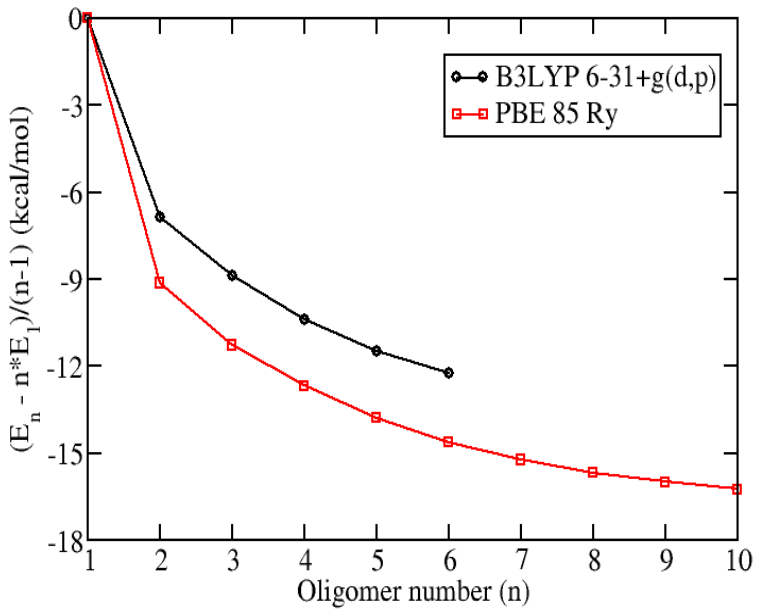

Figure 2.2 Comparison of stabilization energy of oligomers of **1** obtained using B3LYP/6-31+g(d,p) and PBE/85Ry levels of theory.

Factors contributing to the stability of the BTA stacks include hydrogen bonding, π-π and van der Waals interactions.[39] A recent work has examined DFT and DFT-D methods to describe the distance dependence of hydrogen bonding interactions in bimolecular complexes.[40] Post Hartree-Fock methods such as the Møller-Plesset perturbation theory (MP2) are expected to better capture these interactions.

Geometry optimization at the MP2/6-31+g(d,p) level of theory for the BTA dimer yielded a counterpoise-corrected SE of -19.07 kcal/mol. This is in contrast to the value of -6.84 kcal/mol for the dimer at B3LYP 6-31+g(d,p) level of theory. At least a part of the energy deficit in the DFT (B3LYP) calculations could likely be due to the inadequate treatment of dispersive interactions. However, MP2 calculations of higher oligomers is computationally expensive. In order to arrive at reliable estimates of SE and geometry for higher oligomers, density functional theory calculations augmented by the inclusion of empirical van der Waals corrections have been carried out. The parameters of these correction terms for the PBE functional were from Williams and Malhotra.[41]

Geometries of BTA oligomers were optimized with empirical vdW correction added on top of the PBE functional. The resulting stabilization energies are shown in Figure 3. An independent self-consistent field calculation on the optimized configuration carried out without the van der Waals corrections yielded the contribution of DFT to the total SE. The difference between the total SE and the DFT value is the van der Waals contribution to stabilization. Figure 2.3 shows that the van der Waals contribution is quite large for small oligomers, however it decreases and plateaus off for higher one. The intermolecular distance in small oligomers is short (~3.4 Å), resulting in a larger van der Waals stabilisation energy. This distance increases to a value of around

3.7 Å for higher oligomers leading to a slightly reduced van der Waals contribution to the stabilization energy.

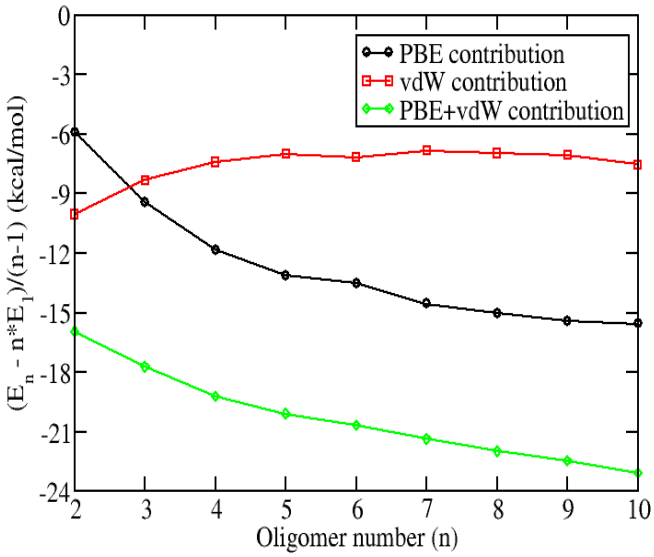

Figure 2.3 Contributions to the stabilization energy of oligomers as a function of their size n using PBE/85 Ry.

Fitting the data in Figure 2.3 to polynomial functions, "bulk" SE values for PBE contribution is found to be about -18.85 kcal/mol and that of the total SE to be about -27.07 kcal/mol. Thus, around -8.2 kcal/mol of the SE comes from vdW interaction.

Figure 2.4 Optimized configuration of BTA tenmer. Faint blue lines denote hydrogen bonds. Side and top view respectively.

As a representative example, the molecular geometries of the tenmer of **1** seen from two different views are shown in Figures 2.4. The geometrical parameters like $r_{N....O}$ distance i.e distance between nitrogen of one molecule and the corresponding hydrogen bonded oxygen of next molecule for tenmer using PBE/85 Ry without vdW correction is 2.88 Å, this is comparable to the value of 2.95 Å obtained by de Greef and coworkers[23] using the same functionals for an infinite chain of trimethyl substituted BTA.

One way to characterize the intermolecular stacking is to observe the twist angles i.e. the angles between the amide carbonyl plane (O-$C_{carbonyl}$-C_{Ar}) and the benzene plane ($C_{carbonyl}$-C_{Ar}-C_{Ar}) is designates as angle (O-$C_{carbonyl}$-C_{Ar}-C_{Ar}), hydrogen bonded H-N plane (H-N-C_{Ar}) and the benzene plane (N-C_{Ar}-C_{Ar}) is designated as (H-N-C_{Ar}-C_{Ar}) and that between the non-hydrogen bonded H_1-N plane (H_1-N-C_{Ar})and the benzene plane (N-C_{Ar}-C_{Ar}) is desingates as (H_1-N-C_{Ar}-C_{Ar}). For tenmer, these twist angles for the core region are found to be approximately 42.26^0, 46.00^0 and 40.8^0, using PBE/85 Ry with van der Waals correction. These values are in agreement (Table 2.1) with reported values for BTA derivative in solid state.[8] Also the average of all the three dihedral angles i.e 40.96^0 for BTA tenmer using PBE/85 Ry without van der Waal correction is comparable to the value of 40.5^0 obtained at the same level of theory for an infinite chain of trimethyl substituted BTA.[23]

Molecule	Twist angle O-$C_{carbonyl}$-C_{Ar}-C_{Ar} (degree)	Twist angle H-N-C_{Ar}-C_{Ar} (degree)	Twist angle H_1-N-C_{Ar}-C_{Ar} (degree)
Benzene-1,3,5-tricarboxamide (**1**) (This calculation)	42.26	46	40.8
1,3,5-N,N',N''-tris(2-methoxyethyl) trimesic amide[8]	36.8	42.4	45.5

Table 2.1 Comparison of twist angles obtained from calculated structures for octamer of **1** with experimental observations.

2.3.2. Co-operativity

An important feature of supramolecular aggregates which emerges from these calculations is cooperativity. Cooperativity captures the influence that a third molecule exerts on the interaction between a pair of molecules.[42]

Here we examine co-operativity in light of the subtle, but systematic changes observed in various geometrical parameters in the core region of the oligomers obtained using PBE/85 Ry with van der Waals correction.

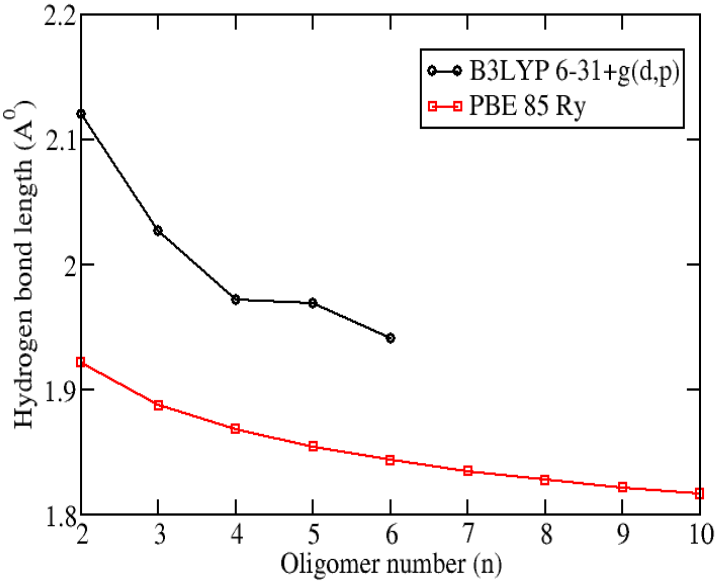

Figure 2.5 Variation of hydrogen bond length in the core region of the oligomers as a function of its size.

The hydrogen bonding between the oxygen of the carbonyl of one molecule and the hydrogen of the amide group belonging to its neighbour is a key element in oligomerization. The length of the hydrogen bond between the molecules in the central (or, core) region of a oligomer is plotted as a function of oligomer size in Figure 2.5. The HB length of the core unit decreases monotonically with increasing oligomer size, from an initial value of 1.93 Å to a converged value of 1.78 Å. This gradual change (albeit for small oligomer sizes) is a manifestation of cooperativity – as monomers are added, intermolecular distances in the core region of the oligomer shorten. The HB lengths obtained from the two methods follow similar trends and are comparable to the experimentally determined HB length of 2.09 Å in 1,3,5-N,N',N''-tris(2-methoxyethyl)trimesic amide.[8] The HB lengths for another derivative of **1** in solid state is also around 2.06 Å.[5] Thus the slight deviation of HB length from the experimental values can be attributed to the presence of alkyl substitutents in the experimentally studied molecules when compared to hydrogen (H_1) in **1**.

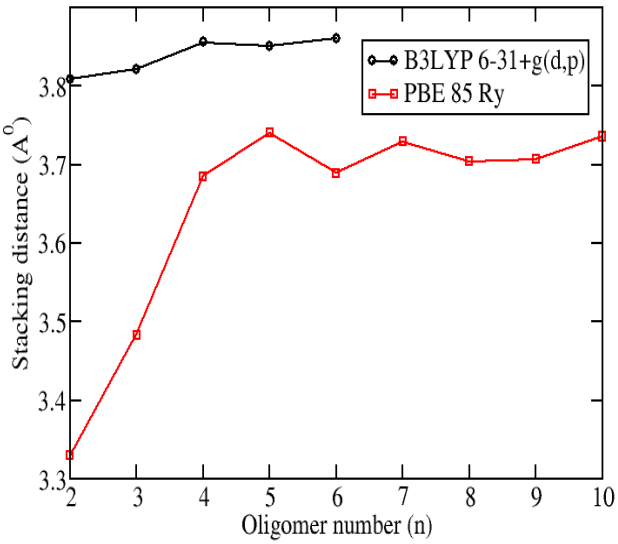

Figure 2.6 Changes in π-π stacking distance in the core region of the oligomers.

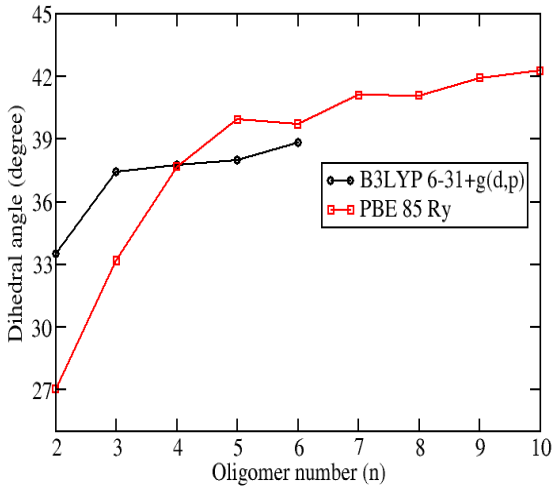

Figure 2.7 Dihedral angle O-$C_{carbonyl}$-C_{Ar}-C_{Ar} as a function of oligomer size (n)

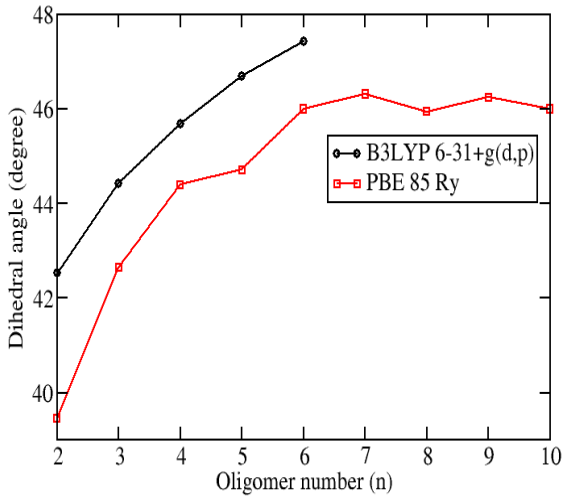

Figure 2.8 Dihedral angle N-H-C_{Ar}-C_{Ar} as a function of olgomer size (n)

A steep increase of about 0.15 Å and 0.20 Å in the π-π stacking distance (Figure 2.6) is observed when we move from the dimer to the trimer and the trimer to the tetramer respectively; however for larger oligomers, the rate of increase is subdued. This observation indicates that the HB

becomes stronger due possibly to the increase in the HB angle towards the ideal value of 180^0. We can see that these distances are also in good agreement with experimental stacking distances of 3.62 Å[8] although a slight change is observed between the two methods.

It may be recalled that although the monomer is planar, a non-zero twist angle is set between the amide plane and the benzene ring plane in larger oligomers. Thus the nature of the change of this twist angle is important from the point of view of cooperativity. From Figures 2.7 and 2.8, we can see that these dihedral angles increase steeply as a function of oligomer number similar to the behaviour exhibited by the stacking distance. The converged values of the dihedral angles are also in good agreement with experimental values of 36.8^0, and 42.4^0.[8]

Thus far, we examined **1** and how the different structural quantities of its oligomers exemplify the evolution of cooperativity. Molecule **2** too belongs to the family of BTA, however, it is capable of forming intramolecular hydrogen bonds. Hence, oligomers of **2** will be devoid of intermolecular hydrogen bonds; thus the only intermolecular interactions in **2** will be π-π stacking and dispersion. If intermolecular hydrogen bonding were a primary determinant of cooperativity, oligomers of **2** should lack the same. How does the stabilisation energy and intermolecular structure evolve for oligomers of **2**? Electronic structure based calculations of **2** reveal a lack of cooperativity in the process of its oligomerization. The SE for oligomers of **2** is not only low (Figure 2.9) but it is nearly independent of the size of the oligomer. The addition of another molecule to a stack does further stabilise the stack but by a constant amount. This manner of aggregation is termed in the literature as isodesmic or step-wise growth. This observation is in agreement with the experimental result from Meijer's group[43] in which a large disc BTA possessing intramolecular hydrogen bonds shows an isodesmic mechanism of self assembly rather than a

cooperative one, a noteworthy fact is that the hydrogen bond donor and the acceptor atoms in **2** is different from that reported in.[43]

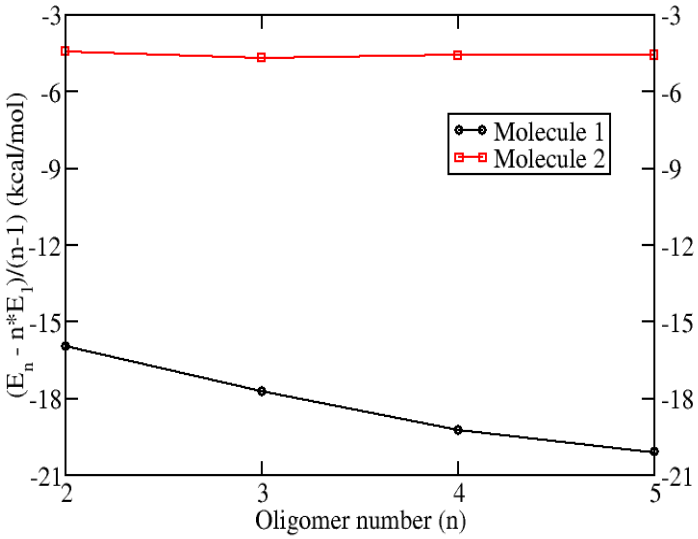

Figure 2.9 Comparison of the evolution of stabilisation energies for molecules **1** and **2**, obtained using PBE functional with empirical vdW correction.

2.3.3 Force field calculations

While quantum chemical calculations are useful in capturing intermolecular interactions and the changes they bring about in intramolecular conformations, they have a high computational demand. In future, molecular modelling efforts on these supramolecular aggregates will likely employ empirical force fields, using which much larger oligomers in vacuum and more importantly, in solution can be studied. It is thus crucial to see how far current force fields are able to reproduce some of the results obtained here using quantum chemical methods. In a preliminary investigation of oligomers of **1**, we have employed the CHARMM generalised force field[32] with atom charges changed to the Mulliken charges obtained from the B3LYP calculation of the

monomer. The revision in the charges was necessary as geometry optimization of the dimer with the original charges of the CHARMM force field for these atom types led to unrealistic geometries in which amide groups of the two molecules faced each other. The use of charges obtained from the B3LYP calculations did not suffer from this handicap and was thus used in further force field based calculations. The SE for small oligomers obtained from these force field based calculations are in good agreement with those calculated using the PBE functional augmented with the empirical vdW correction. The SE decreases further for higher oligomers and saturates for oligomer sizes in the range of 25-30 molecules (Figure 2.10). By fitting the SE to a polynomial in n, a bulk value of -24.3 kcal/mol is obtained.

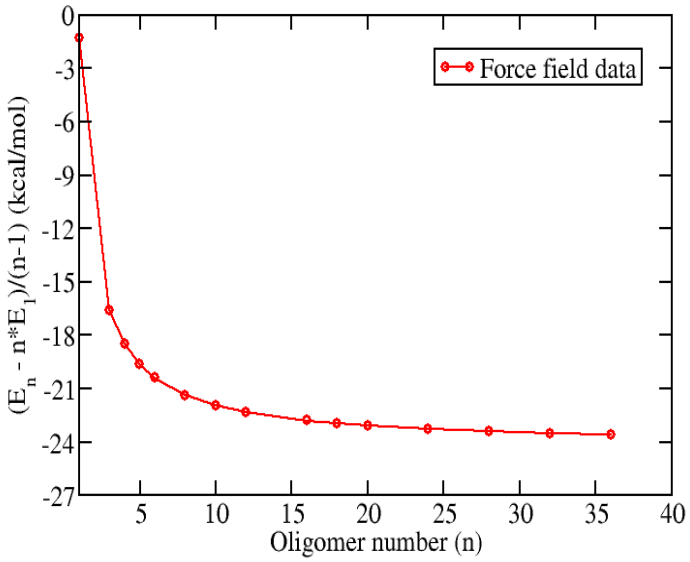

Figure 2.10 Stabilization energy as a function of oligomer size using force field.

2.3.4 Dipole moment

Another noteworthy feature of the stacks of **1** is the enormous increase in the dipole moment of the oligomer as its size increases, manifesting in high surface potentials observed experimentally using Kelvin probe microscopy.[9] It arises from the directionality and alignment of the hydrogen bonds along the long axis of the stack. The dipole moment component along the long axis of the hydrogen bonds add to give rise to a macrodipole for the oligomer. The contribution to this dipole moment of the oligomer from each of the molecule increases with oligomer size and saturates to a value of 12.35 D (Figure 2.11 (a)) as obtained from the PBE/85 Ry calculations. The corresponding value from the force field calculations is around 8 D (Figure 2.11(b)). Thus, the empirical calculations agree qualitatively with the quantum chemical results, and provides pointers in the process of further refinement of the potential parameters. The large macrodipole also helps to explain the fact that these stacks come together to form bundles or fibers in apolar solvents[5] because of the macrodipole-macrodipole interaction leading to further stabilisation of the assembly.

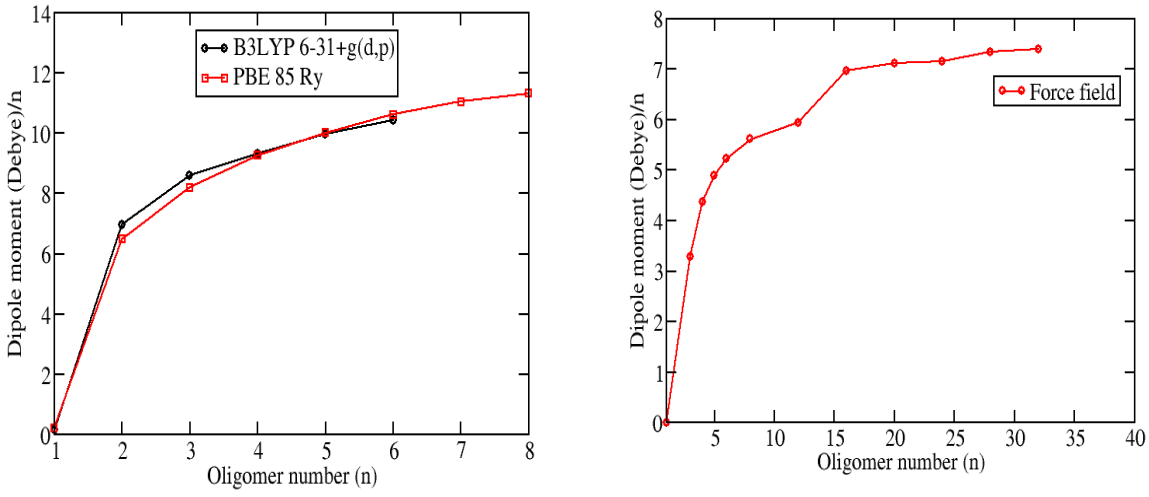

(a) (b)

Figure 2.11 Mean dipole moment per molecule as a function of oligomer size for molecule **1** (a) DFT calculation (b) Force field calculation.

In the case of molecule **2**, the calculated dipole moment values are much lower and independent of the oligomer size (Table 2.2), due primarily to the planarity of **2** imposed by the presence of three intramolecular hydrogen bonds. Through an elegant analysis, de Greef and coworkers[23] have shown recently that the contribution from molecular dipole-dipole interactions to the stabilization energy is around 43%. We concur with this argument.

Oligomer size (n)	Dipole moment of oligomers of molecule **1** (Debye)	Dipole moment of oligomers of molecule **2** (Debye)
Monomer	0.21	0.56
Dimer	12.98	0.05
Trimer	24.58	0.58
Tetramer	37.07	0.14
Pentamer	50.06	0.58

Table 2.2 Comparison of dipole moment of oligomers of molecules **1** and **2**.

2.3.5 Free energy calculations

While the changes in different parameters of the central hydrogen bond indicate the cooperativity, the evolution of change in Gibbs free energy (ΔG) as a function of oligomer size can differentiate between different types of cooperativity i.e. nucleation-elongation or cooperative downhill polymerisation. Since change in Gibbs free energy (ΔG) includes contributions from entropy and temperature along with the internal energy of the system, it provides a more accurate picture of the mechanism of supramolecular polymerisation operating in the system.

For molecule **1** we have calculated the change in Gibbs free energy ($\Delta G=G_n-n*G_1$) as a function of oligomer size at different temperatures (Figure 2.12). The Gibbs free energy contains contributions from the vibrational, rotational, translational degrees of freedom to the entropy and to the finite temperature internal energy. Beyond 400 K, the aggregates are no longer stable because ΔG remains positive for all oligomers studied. For all temperatures below 400 K, the ΔG initially dips down and peaks at tetramer and after tetramer it starts to decrease again. At temperatures of 370 K and 380 K the ΔG becomes positive for tetramer and then decreases. This suggests that some kind of barrier exists for the polymerisation till it reaches tetramer and beyond that it grows spontaneously (ΔG is negative) at temperatures of 370 K and 380 K. This is similar to the cooperative nucleation-elongation mechanism which involves a ΔG barrier till the formation of nucleus and after that it grows spontaneously. But for a cooperative nucleation-elongation mechanism of polymerisation, ideally an increase in ΔG should be seen till the aggregate reaches the nucleus, but in our simulation results we see a small dip initially, followed by a rise till tetramer and beyond that ΔG is negative. Thus the mechanism seems to be cooperative nucleation-elongation and the initial dip in ΔG can be attributed to the rudimentary nature of the force field which is being employed in this study. Experimental observations indicate the formation of aggregates in the temperature range of 350 K to 360 K depending on the concentration of the solution.[13] Thus a fair degree of agreement can be seen between the experimental and the simulation results with respect to the temperature at which aggregation begins. These preliminary results, based on the force field provides us confidence on this line of approach. A quantitative comparison to experimental results on the aggregation mechanism demands further refinement of the generic force field to the specific molecule. This is the objective of our future studies in this area.

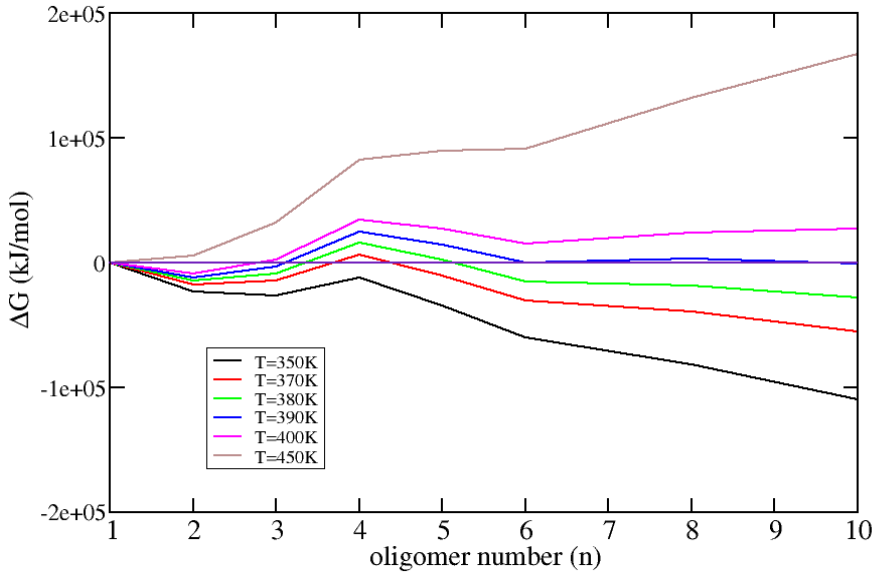

Figure 2.12 Change in Gibbs free energy as a function of oligomer number for molecule **1**.

2.4 Conclusions

Here, we have examined the supramolecular organization of two simple compounds in the benzene tricarboxamide family using, primarily quantum chemical calculations and using a force field. The bulk stabilization energy of a stack of **1** is estimated to be around -27.07 kcal/mol using PBE/85Ry level of theory. Empirical force field based calculations yield a corresponding value of -24.3 kcal/mol. The formation of three intermolecular hydrogen bonds is a crucial step in the oligomerization of BTA. However, pair interactions are seen to be further stabilized by the presence of other molecules in the aggregate – a feature termed, cooperativity. The presence of intramolecular hydrogen bonds in molecule **2** is shown to lead to a lack of cooperativity in its oligomerization. Thus, while molecule **1** is predicted to show a nucleation and growth type of self assembly, molecule **2** is indicated to follow an isodesmic model of self-assembly, which is in

accord with experimental observations. van der Waals interactions contribute a siginificant amount (about -8 kcal/mol) to the total stabilization energy for molecule **1**. The stabilization energy in the force field calculations saturate for an oligomer containing around 30 molecules. The evolution of change in Gibbs free energy as a function of oilgomer size indicates a cooperative nucleation-elongation mechanism of polymerisation.

2.5 Future outlook

With the further refinement of the present force field, it can be used to study the mechanisms of self-assembly in solution, using molecular dynamics simulations. Also the synthesis and study of self-assembly mechanisms of molecule **2** is presently under way. In order to assign the mechanisms of self-assembly based on the change in Gibbs free energy unambiguously, quantum chemical approaches to calculation of change in Gibbs free energy are presently being pursued.

2.6 References

1. de Greef, T. F. A.; Smulders, M. M. J.; Wolffs, M.; Schenning, A. P. H. J.; Sijbesma, R. P.; Meijer, E. W. *Chem. Rev*. **2009**, *109*, 5687.
2. Brunsveld, L.; Folmer, B. J. B.; Meijer, E. W.; Sijbesma, R. P. *Chem. Rev.* 2001, 101, 4071.
3. Palmans, A. R. A.; Meijer, E. W. *Angew. Chem. Int. Ed.* **2007**, *46*, 8948.
4. Wilson, A. J.;van Gestel, J.; Sijbesma, R. P.; Meijer, E. W. *Chem. Commun.* **2006**, 4404.
5. Bose, P. P.; Drew, M. G. B.; Das, A. K.; Banerjee, A. *Chem. Commun.* **2006**, 3196.
6. Mes, T.; Smulders, M. M. J.; Palmans, A. J. A.; Meijer, E. W. *Macromolecules* **2010**, *43*, 1981.
7. Jimenez, C. A.; Belmar, J. B.; Oritz, L.; Hidalgo, P.; Fabelo, O.; Pasan, J.; Ruiz-Perez, C.; *Cryst. Growth Des.* **2009**, *9*, 4987.
8. Lighthood, M. P.; Mair, F. S.; Pritchard, R. G.; Wareen, J. E. *Chem. Commun.* **1999**, 1945.
9. Fitie, C. F. C.; Christian Roelofs, W. S.; Kemerink, M.; Sijbesma, R. P. *J. Am. Chem. Soc*. **2010**, *132*, 6892.
10. Stals, P. J. M.; Smulders, M. M. J.; Martin-Rapun, R.; Palmans, A. R. A.; Meijer, E. W. *Chem. Eur. J.* **2009**, *15*, 2071.
11. Danila, I.; Riobe, F.; Pugimarti-Luis, J.; de Pino, A. P.; Wallis, J. D.; Ambilino, D. B.; Avarvari, N. *J. Mater. Chem.* **2009**, *19*,4495.
12. Roosma, J.; Mes, T.; Leclere, P.; Palmans, A. R. A.; Meijer, E. W. *J. Am. Chem. Soc.* **2008**, *130*, 1120.
13. Smulders, M. M. J.; Schenning, A. P. H. J.; Meijer, E. W. *J. Am. Chem. Soc*. **2008**, *130*, 606.
14. Smulders, M. M. J; Filot,.I. A. W.; Leenders, J. M. A.; van der Schoot, P.; Palmans, A. R. A.; Schenning, A. P. H. J.; Meijer, E. W. *J. Am. Chem. Soc.* **2010**, *132*, 611.

15. van Gestel, J.; Palmans, A. R. A.; Titulaer, B.; Vekemans, Jef A. J. M.; Meijer, E. W. *J. Am. Chem. Soc.* **2005**, *127*, 5490.

16. Smulders, M. M. J.; Stals, P. J. M.; Mes, T.; Paffen, T. F. E.; Schenning, A. P. H. J.; Palmans, A. R. A.; Meijer, E. W. *J. Am. Chem. Soc.* **2010**, *132*, 620.

17. van Gestel, J.; van der Schoot, P.; Michels, M. A. J. *Macromolecules* **2003**, *36*, 6668.

18. van Gestel, J.; *Macromolecules* **2004**, *37*, 3894.

19. Bushey, M. L.; Hwang, A.; Stephens, P. W.; Nuckolls, C. *J. Am. Chem. Soc.* **2001**, *123*, 8157.

20. Rochefort, A.; Bayard, E.; Hadj-Messaoud, S. *Adv. Mater*. **2007**, *19*, 1992.

21. Bushey, M. L.; Hwang, A.; Stephens, P. W.; Nuckolls, C. *Angew. Chem. Int. Ed.* **2002**, *41*, 2828.

22. Bayard, E.; Hamel, S.; Rochefort, A. *Organic Electronics* **2006**, *7*, 144.

23. Filot, I. W. A.; Palmans, A. R. A.; Hilbers, P. A. J.; van Santen, R. A.; Pidko, E. A.; de Greef, T. F. A. *J. Phys. Chem. B*, **2010**, *114*, 13667.

24. Frisch,M. J. et al *Gaussian-03*, *Gaussian Inc*.; Pittsburgh, PA, **2003**.

25. Sim, F.; St-Amant, A.; Papai, I.; Salhub, D. R. *J. Am. Chem. Soc.* **1992**, *114*, 4391.

26. Pudzianowski, A. T. *J. Phys. Chem.* **1996**, *100*, 4781.

27. Perdew, J.P.; Burke, K.; Emzerhof, M. *Phys. Rev. Lett.* **1996**, *77*, 3865 .

28. Hutter, J.; Ballone, J. P.; Bernasconi, M.; Focher, P.; Fois, E.; Goedecker, S.; Marx, D.; Parrinello, M.; Tuckermann, M. E. CPMD version 3.13.2, Max Planck Institut fuer Festkoerperforschung, Stuttgart, and IBM Zurich Research Laboratory, **1990**-.

29. Hockney, R. W. *Methods Comput. Phys.* **1970**, *9*, 136.

30. Shapere,A. and Wilczek, F. Eds., *Geometric Phases in Physics;* World Scientific; Singapore; **1989.**

31. Plimpton, S. J. *J. Comp. Phys.* **1995**, *117*, 1. http://lammps.sandia.gov

32. Vanommeslaeghe, K.; Hatcher, E.; Acharya, C.; Kundu, S.; Zhong, S.; Shim, J.; Darian, E.; Guvench, O.; Lopes, P.; Vorobyov, I.; Mackerell Jr., A. D. *J. Comput. Chem.* **2010**, *31*, 671.

33. Humphrey, W.; Dalke, A.; Schulten, k. *J. Molec. Graphics* **1996**, *14*, 33.

34. Jakubikova, E.; Rappe, A. K.; Bernstein, E. R. *J. Phys. Chem. A* **2006**, *110*, 9529.

35. Riley, K. E.; Pitonak, M.; Jurecka, P.; Hobza, P. *Chem. Rev.* **2010**, *110*, 5023.

36. Khaliullin, R. Z.; Cobar, E. A.; Lochan, R. C.; Bell, A. T.; Head-Gordon, M. *J. Phys. Chem. A* **2007**, *111*, 8753.

37. Zaho, Y.; Truhlar, D. G. *J. Chem. Theory Comput.* **2005**, *1*, 415.

38. Tasoni, S.; Tuma, C.; Sauer, J.; Civalleri, B.; Ugliengo, P. *J. Chem. Phys.* **2007**, *127*, 154102.

39. Grimme, S. *Angew. Chem. Int. Ed.* **2008**, *47*, 3430.

40. Thanthiriwatte, K. S.; Hohenstein, E. G.; Burns, L. A.; Sherrill, C. D. *J. Chem. Theory Comput.* **2011**, *7*, 88.

41. Williams, R. W.; Malhotra, D. *Chemical Physics* **2006**, *327*, 54.

42. Hunter, C. A.; Anderson, H. L. *Angew. Chem. Int. Ed.* **2009**, *48*, 7488.

43. Metzroth, T.; Hoffmann, A.; Martin-Rapun, R.; Smulders, M. M. J.; Pieterse, K.; Palmans, A. R. A.; Vekemans, Jef A. J. M.; Meijer, E. W.; Spiess, H. W.; Gauss, J. *Chem. Sci.* **2011**, *2*, 69.